TABLE OF CONTENTS

	PAGE
ABSTRACT	i
ACKNOWLEDGMENTS	ii
LIST OF FIGURES	iii
LIST OF TABLES	vi
NOMENCLATURE	vii
INTRODUCTION	1
LITERATURE REVIEW	3
Experimental Methods	4
Correlation Methods and Prediction Methods	7
EXPERIMENTAL DETAILS	10
The Equilibrium Cell	10
Cryostat, Its Temperature Control System and Measurement System	10
The Electromagnetic Pump	14
Pressure Measurement	14
The Recirculation Loop	14
Evacuation of the Feeding Devices	15
Material	15
Experimental Procedure	16
Analytical Method	16
RESULTS AND CORRELATION OF DATA	19

PAGE

DISCUSSION AND CONCLUSION 45

Nitrogen-Methane Mixtures 45

Nitrogen-Ethane Mixtures 45

Nitrogen-Methane-Ethane Mixtures 46

APPENDIX I

Experimental and Smooth Data of the Systems Containing Nitrogen, Methane and Ethane 48

APPENDIX II

Calibration Results for the Thermocouple 68

APPENDIX III

Calibration Curves 70

BIBLIOGRAPHY 73

ABSTRACT

Phase equilibrium compositions were measured by means of a forced-recirculation equilibrium cell for the binary and ternary mixtures of nitrogen, methane and ethane from -255° to -153.1°F and the pressures up to 709 psia.

At temperatures lower than -218°F, two liquid phases were observed for the nitrogen-ethane binary and for the nitrogen-methane-ethane ternary systems. This phenomenon occurred when the methane concentration in the liquid phase was less than 17 mole percent.

K values for the components in binary and ternary systems were correlated as a function of pressure and composition at isothermal conditions. For the ternary system, correlations were made using $x_{CH_4}/(x_{CH_4} + x_{C_2H_6})$ as the parameter. Liquid-liquid equilibrium compositions were correlated in terms of distribution coefficients and a solubility function.

ACKNOWLEDGEMENT

The author is very much indebted to Dr. Benjamin C.-Y. Lu for directing this research work, for his guidance and encouragement in every phase, and for his readiness to discuss problems.

Mr. S.D. Chang, a senior graduate student in the department, helped in setting up the apparatus and gave helpful suggestions.

Mr. D. Gravelle, a graduate student in the department, helped in taking part of data.

The author is very grateful to Messrs. F. Giacobbi, J. Gasperetti and G. Grunet for their technical assistance.

Dr. S.S. You read the manuscript and made grammatical corrections.

LIST OF FIGURES

FIGURE		PAGE
1.	A Schematic Flow Diagram of the Forced-Recirculation Apparatus	11
2.	A Schematic Diagram of Equilibrium Cell and the Cryostat	13
3.	Chromatogram of run 1805	18
4.	The P-X-Y Diagram of the Nitrogen-Methane System at -216.3°F	21
5.	The P-X-Y Diagram of the Nitrogen-Methane System at -225.5°F	22
6.	The P-X-Y Diagram of the Nitrogen-Ethane System at -159.1°F	23
7.	The P-X-Y Diagram of the Nitrogen-Ethane System at -225.5°F	24
8.	The K-P Diagram of the Nitrogen-Methane System	25
9.	The K-P Diagram of the Nitrogen-Ethane System	26
10.	Equilibrium Composition Diagram for the Nitrogen-Methane-Ethane System at -225.5°F and X_{e_1}/X_{e_2} = 0.14	27
11.	Equilibrium Composition Diagram for the Nitrogen-Methane-Ethane System at -225.5°F and X_{e_1}/X_{e_2} = 0.30	28
12.	Equilibrium Composition Diagram for the Nitrogen-Methane-Ethane System at -225.5°F and X_{e_1}/X_{e_2} = 0.47	29

FIGURE		PAGE
13.	Equilibrium Composition Diagram for the Nitrogen-Methane Ethane System at -225.5°F and X_{c_1}/X_{c_2} = 1.27	30
14.	Equilibrium Composition Diagram for the Nitrogen-Methane Ethane System at -225.5°F and X_{c_1}/X_{c_2} = 2.33	31
15.	The log K-P Diagram for the Nitrogen-Methane-Ethane System at -225.5°F, using $X_{c_1}/(X_{c_1} + X_{c_2})$ as Parameter	32
16.	Liquid-Liquid-Vapour Equilibria for the Nitrogen-Methane-Ethane System at -225.5°F	33
17.	Liquid-Liquid-Vapour Equilibria for the Nitrogen-Methane-Ethane System at -250°F	34
18.	Liquid-Liquid-Vapour Equilibria for the Nitrogen-Methane-Ethane System at -255°F	35
19.	Change of Composition of the Three Co-existing Phases with Temperature for the Nitrogen-Ethane System	36
20.	Correlation of the Solubility Function, K'_H with the Liquid-Liquid Distribution Coefficient K'_{N_2}	37
21.	Correlation of the Solubility Function, K'_{c_1} with the Liquid-Liquid Distribution Coefficient K'_{N_2}	38
22.	Correlation of the Solubility Function, K'_{c_2} with the Liquid-Liquid Distribution Coefficient K'_{N_2}	39

FIGURE		PAGE
23.	Correlation of the Solubility Function K'_H with Temperature	40
24.	Correlation of the Solubility Function, K'_{c_1} with Temperature	41
25.	Correlation of the Solubility Function, K'_{c_2} with Temperature	42
26.	The K_{N_2}-P Diagram for the Nitrogen-Methane-Ethane System in the Three-Phase Region	43
27.	The K_{c_1}-P Diagram for the Nitrogen-Methane-Ethane System in the Three-Phase Region	44
28.	Calibration Results of the Thermocouple	69
29.	Calibration Curves for the Binary and the Ternary Mixtures	71
30.	Calibration Curves for the Binary and the Ternary Mixtures	72

LIST OF TABLES

TABLE		PAGE
I	Experimental Data for the System Nitrogen-Methane	49
II	Experimental Data For The System Nitrogen-Ethane	50
III	Smoothed Data For The System Nitrogen-Methane	51
IV	Smoothed Data For The System Nitrogen-Ethane	52
V	Experimental Data For The Ternary System Nitrogen-Methane-Ethane at Temperature -225.5°F	54
VI	K Values For The Ternary System Nitrogen-Methane-Ethane at Temperature -225.5°F	57
VII	Experimental Data For The Ternary System Nitrogen-Methane-Ethane Containing Two Liquid Phases	60
VIII	K Values and Distribution Coefficients For the Ternary System Nitrogen-Methane-Ethane Containing Two Liquid Phases	64

NOMENCLATURE

BL = bottom layer of liquid phase.

^{o}C = degrees Centigrade.

^{o}F = degrees Fahrenheit.

f = fugacity.

K = equilibrium constant.

K'_H = distribution coefficient for the total hydrocarbon material between the two liquid phases.

K'_1 = distribution coefficient defined as $x_1(BL)/x_1(TL)$, the distribution coefficient.

P = total pressure on system.

P_i = partial pressure of ith species.

R = gas constant per mole.

T = temperature.

TL = top layer of liquid phase.

x_i = mole fraction of the component i in liquid phase.

y_i = mole fraction of the component i in vapour phase.

γ_i = activity coefficient of component i.

ϕ_i = $\frac{f_i}{x_i P}$, fugacity coefficient of component i in the solution.

μ_i = chemical potential of component i.

μ_i^o = Gibbs free energy per mole of pure substance at unit pressure, and at the same temperature as that of the mixture under discussion.

α = $\frac{x_{c_1}}{x_{c_1} + x_{c_2}}$, the third parameter of correlations.

Subscripts

1

2

c_1 = methane

c_2 = ethane

H = hydrocarbon

1

Superscripts

$\wedge$ = molal property in the mixture.

v = vapour phase.

l = liquid phase.

Subscripts

1

2

c_1 = methane

c_2 = ethane

H = hydrocarbon

1

Superscripts

$\wedge$ = molal property in the mixture.

v = vapour phase.

l = liquid phase.

INTRODUCTION

In the separation of natural gases into components or the removal of non-combustible from natural gases, phases equilibrium data are necessary for the design of the separation equipment. Natural gases usually contain light hydrocarbon such as methane and ethane, and nitrogen, hydrogen or helium as impurities.

Although phase equilibrium data are available in the literature for binary mixtures of nitrogen-methane, methane-ethane, and ethane-nitrogen (1 to 10), few determinations have been made on ternary mixtures of these components (3,10).

Phase equilibrium data may be obtained experimentally or by prediction. Prediction methods have been developed by evaluating activity or fugacity coefficients, with the help of a suitable equation of state. However, a suitable equation of state is not available for both vapour and liquid phases over a wide range of temperature and pressure. For example, one of the best known equations of state, the Benedict-Webb-Rubin equation may be used, in general, to predict vapour-liquid equilibrium, but it has been recognized even by Benedict himself that at low temperature it is not entirely satisfactory (11). Therefore, it may be concluded that to date no single method has been successful in describing all the binary and ternary vapour-liquid equilibrium systems.

In order to get acquainted with the experimental technique and to test the performance of the apparatus, determination of binary vapour-

liquid equilibrium data were made at three isothermal conditions -225.5, -216.3 and -153.1°F for the nitrogen-methane and nitrogen-ethane systems.

For the ternary system, vapour-liquid equilibrium data were determined at -225.5°F. At -240°F, two liquid phases were observed in equilibrium with vapour phase for nitrogen-ethane binary and nitrogen methane-ethane ternary systems (10). The existence of two liquid phases at the low temperature is particularly interesting, because the separation of nitrogen from natural gases rich in nitrogen may be facilitated by taking advantage of composition differences of the two liquid phases. For this reason, three more isotherms of liquid-liquid-vapour equilibrium were measured for nitrogen-ethane binary and nitrogen-methane-ethane ternary system.

LITERATURE REVIEW

Few phase equilibrium data were available in the literature for natural gases at low temperatures. The systems which have been studied are listed below:

System	Source
Helium-nitrogen	(12)
Argon-oxygen	(13)
Argon-nitrogen	(14)
Methane-ethylene	(15,16)
Methane-ethane	(1,2,17,18)
Methane-propane	(19,17)
Methane-n-butane	(20)
Methane-carbon monoxide	(21)
Nitrogen-methane	(1,2,9,10,21)
Nitrogen-propane	(21)
Nitrogen-ethane	(3 to 10)
Nitrogen-carbon monoxide	(22)
Ethylene-ethane	(23)
Ethylene-propane	(24,25)
Ethylene-propylene	(25)
Methane-ethylene-ethane	(26)
Methane-ethane-propane	(7)

System	Source
Nitrogen-methane-ethane	(3,10)
Nitrogen-propane-propene	(21)
Ethylene-ethane-acetylene	(25)

The above review of literature reveals only meager data on vapour liquid equilibria of the nitrogen-methane-ethane system at low temperature.

In this study, a brief review of literature will be made concerning the experimental procedure and methods of correlation and prediction.

EXPERIMENTAL METHODS

Methods for the direct determination of vapor-liquid equilibrium data can be classified as follows

(1) Distillation method.

(2) Dew and Bubble point method.

(3) Static method.

(4) Flow method.

(5) Forced-recirculation method.

The Distillation Method

The oldest method for direct determination of vapour-liquid equilibrium data is the distillation method in which a small amount of liquid is distilled off from the boiling flask containing a large charge.

System	Source
Nitrogen-methane-ethane	(3,10)
Nitrogen-propane-propene	(21)
Ethylene-ethane-acetylene	(25)

The above review of literature reveals only meager data on vapour liquid equilibria of the nitrogen-methane-ethane system at low temperature.

In this study, a brief review of literature will be made concerning the experimental procedure and methods of correlation and prediction.

EXPERIMENTAL METHODS

Methods for the direct determination of vapor-liquid equilibrium data can be classified as follows

(1) Distillation method.

(2) Dew and Bubble point method.

(3) Static method.

(4) Flow method.

(5) Forced-recirculation method.

The Distillation Method

The oldest method for direct determination of vapour-liquid equilibrium data is the distillation method in which a small amount of liquid is distilled off from the boiling flask containing a large charge.

This method was very simple but had marked disadvantages and generated large errors. This method is no longer used today.

The Dew and Bubble Point Method

This method was employed by Sage and Lacy (27,17) for determining phase equilibria of light hydrocarbons in the temperature range from 20° to 100°C. This method was applied by Bloomer and Parent (1,2) at low temperature. In this method the gases of known composition were fed into the equilibrium apparatus. The vapour and liquid samples need not be analyzed. The disadvantage is that the data can be obtained for the binary systems only.

The Static Method

The static method was utilised by Fedoritenko and Ruhemann (12) at low temperature. In this method a mixture of gases is placed in the equilibrium cell and maintained at constant temperature for a long time. Then the samples are taken and analyzed. This method requires an exceptionally long time for reaching the equilibrium condition and may introduce errors during sampling, as the pressure may change from the equilibrium pressure.

The Flow Method

A gas mixture is passed under steady state condition into the equilibrium cell where it is cooled and partially liquified. The samples are withdrawn and analyzed continuously.

This method was utilised by Steckel and Zinn (28) and by Ruhemann and Zinn (29) for determining phase equilibrium data, and by Stutzman and Brown (30) for natural gas at low temperature. The disadvantage lies in the maintenance of constant pressure and temperature during rapid condensation.

The Forced-Recirculation Method

The vapour vapourized from the liquid is recirculated back through the liquid by means of a pump. In this way the liquid was stirred and equilibrium insured by continually bringing the vapour into contact with the liquid.

The forced-recirculation method was developed by Inglis (31) and modified and used by Dodge and Dunbar (32) for the oxygen-nitrogen system. It was used by Torocheshnikov (33) for the carbon monoxide-nitrogen system and modified by Aroyan and Katz (34) for the methane-hydrogen system and in their steady circulation process by employing an electro-magnetic pump. Davis, Rodewald and Kurata (35) modified the equipment further.

It is probably the most accurate and reliable one of all the existing methods and is widely used at present. The advantages of this method are as follows: (1) the equilibrium is reached very quickly, and (2) the vapour and liquid samples can be withdrawn almost without disturbing the equilibrium. For these reasons, this method is utilised in the present investigation.

CORRELATION METHODS AND PREDICTION METHODS

Equilibrium Ratio

The equilibrium ratio is defined as

$$K_i = \frac{y_i}{x_i} \qquad (1)$$

The plots of logarithmic values of equilibrium ratio, as functions of the logarithmic values of the total pressure are frequently used as a means of representation.

Fugacity Coefficients of the Components

The fugacity of the ith component in the mixture at constant temperature is defined as

$$\mu_i = \mu_i^0 + RT \ln \hat{f}_i$$
$$f_i/P_i \to 1 \text{ as } P \to 0 \qquad (2)$$

at equilibrium

$$\mu_i^V = \mu_i^l \qquad (3)$$

so

$$\hat{f}_i^V = \hat{f}_i^l \qquad (4)$$

now

$$\hat{f}_i^V = \hat{\phi}_i^V y_i P \qquad (5)$$

$$\hat{f}_i^l = \hat{\phi}_i^l x_i P \qquad (6)$$

Therefore, from (5) and (6)

$$K_i = \frac{y_i}{x_i} = \frac{\hat{\phi}_i^l}{\hat{\phi}_i^v} \qquad (7)$$

One may therefore evaluate the equilibrium vapourization constant K_i by knowing the fugacity coefficients. The calculation of fugacity coefficients in the both phases of liquid and vapor are not possible at the present stage due to the lack of a suitable equation of state and mixing rule. Hence this method is not employed in this investigation.

Activity Coefficients of the Components

The activity coefficient of the ith component in the solution is defined as:

$$r_i = \frac{\hat{f}_i}{x_i f_i} \qquad (8)$$

or

$$\hat{f}_i^l = r_i^l x_i f_i^l \qquad (9)$$

and

$$\hat{f}_i^v = r_i^v y_i f_i^v \qquad (10)$$

at equilibrium

$$\hat{f}_i^l = \hat{f}_i^v \qquad (11)$$

therefore

$$r_i^l x_i f_i^l = r_i^v y_i f_i^v \qquad (12)$$

$$K_i = \frac{y_i}{x_i} = \frac{r_i^l f_i^l}{r_i^v f_i^v} \qquad (13)$$

By combining the activity and the fugacity coefficients, the following relationship is obtained:

$$\hat{f}_1^v = y_1 \hat{\phi}_1^v p = \hat{f}_1^l = r_1^l x_1 f_1^l \qquad (14)$$

$$k_1 = \frac{r_1^l f_1^l}{\hat{\phi}_1^v p} \qquad (15)$$

This is a convenient relationship to be used for evaluating K values. Since f_1^l, the fugacity of pure component i is generally available, $\hat{\phi}_1^v$ fugacity coefficient of the vapour phase can usually be calculated by using an equation of state.

EXPERIMENTAL DETAILS

An apparatus was built in this study and phase equilibrium data were measured at low temperature and high pressure.

The apparatus shown in the schematic diagram, Fig. 1, consists of the following sections: the equilibrium cell, the low temperature bath, the electro-magnetic pump, the temperature control and measurement system, the pressure measurement, the evacuation and feeding devices and the set of sample facilities.

The Equilibrium Cell

A 100 ml. Jerguson transparent gage with stainless steel body was used as the equilibrium cell. The inside diameter was 3/8 inch and the length was 6 inches. The top end was sealed by a Swagelok connector, through which connected two protective type thermocouples of 1/16 inch in diameter and three 3/16 inch sampling tubings were inserted. The bottom end was welded with an 1/8 inch Autoclave joint which was connected to the cooling coil of the vapour inlet line. A sprayer with twenty tiny holes sprayed the vapour inside the equilibrium cell. Two screens, one near the top and the other near the bottom, were used to reduce entrainment and to distribute the vapour.

Cryostat, its Temperature Control System and Measurement System

A Dewar flask having a capacity of about 20 liters was employed as the cryostat, into which the equilibrium cell was

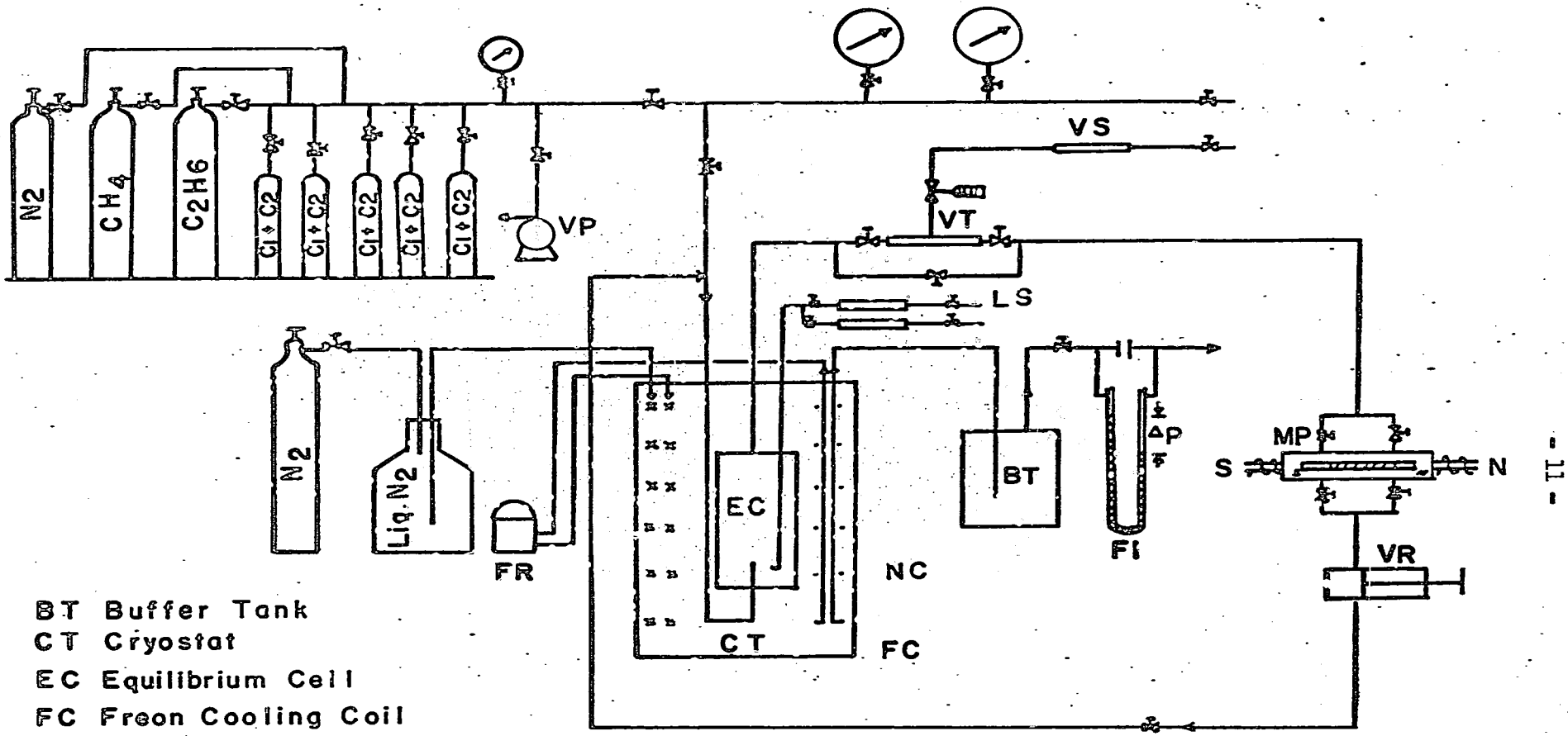

BT Buffer Tank
CT Cryostat
EC Equilibrium Cell
FC Freon Cooling Coil
FI Flow Indicator
FR Freon Compressor
LS Liquid Sampling Bulb
MP Magnetic Pump
NC Nitrogen Vaporization Coil
VP Vacuum Pump
VR Volume Regulator
VS Volume Sampling Bulb
VT Volume Sampling Tube

Figure 1. A schematic flow diagram of the forced-recirculation apparatus.

immersed. In this investigation isopentane was used as the bath liquid. A schematic diagram of the cell and cryostat is shown in Fig. 2.

Inside the cryostat, a refrigeration coil, two stirrers, two heating elements and a resistant type temperature sensing element were installed. Liquid nitrogen was used as the refrigerant which was supplied under pressure through the refrigerant coil. The refrigerant-nitrogen, after vapourization, was led through a five-gallon buffer tank, a needle valve and a manometer and then open to the air. The evaporation rate of liquid nitrogen was controlled by the needle valve and the manometer.

The bath was heated by a pair of heating elements which were connected to the power source through a powerstat. One of them was used as a controlling heater which was connected through the temperature controller. The other was used as a constant heater. A variable speed stirrer was used to stir the bath liquid.

The bath was cooled to a temperature slightly lower than that is desired by regulating the flow of the liquid nitrogen and by adjusting the voltage of one immersion heater. The controlling heater connected through a Bayley temperature controller model 250 with resistance-sensing element maintained the required temperature.

The temperature was measured by two copper constantan thermocouples, one for the vapour phase and one for the liquid phase, in conjunction with a Leeds and Northrup K-3 potentiometer and a Tinsley SR I galvanometer. The reference junction was placed inside a crushed ice bath.

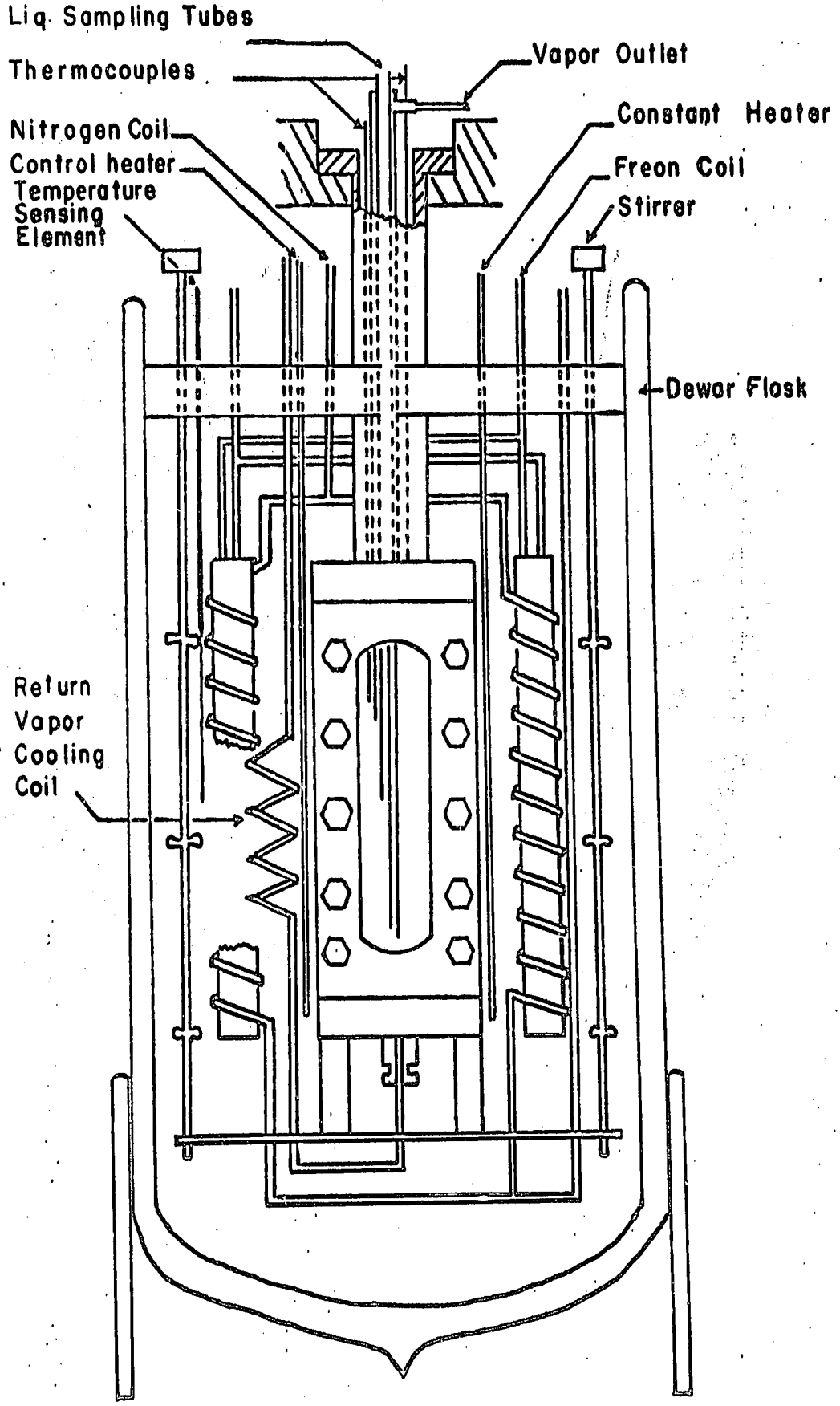

Figure 2. A schematic diagram of equilibrium cell and the cryostat.

The thermocouple was calibrated against the vapour pressure of research grade methane (36) and compared with the conversion table of copper constantan thermocouple (37). Results of the calibration are shown in Appendix II.

The bath temperature was controlled to within [illegible] ± 0.02°F.

The Electromagnetic Pump

For the recirculation of the vapour, an electromagnetic pump was used. The design was based on that reported by Sterner (38) with several modifications which were made by Chang (10).

The pump capacity was 0 to 56 cc. per min. The pressure drop across the pump was 0 to 6.3 psi.

Pressure Measurement

Equilibrium pressure was measured by either one of the two tested Heise gauges. The range of one gauge is 0 - 1000 psia with 1 psi per division and the other, 0 - 2500 psia with 4 psi per division. These gauges have 0.1 percent of maximum hysteresis at 70°F.

The Recirculation Loop

After thermal equilibrium was reached in the cell, the vapour was recirculated within the recirculation loop which, as shown in Fig. 1, consists of the electromagnetic pump and the equilibrium cell, a volume regulator, a sampling loop and a cooling coil. When the vapour passed through the volume regulator and the sampling loop, it was heated up to the room temperature , but it was cooled to the bath temperature when it passed

through the cooling coil inside the cryostat before returning to the equilibrium cell.

Evacuation of the Feeding Devices

The recirculation loop, the sampling tube and pressure gauges were evacuated to one-hundredth of a milimeter mercury before each run by using a vacuum pump. A McLeod gauge was employed to detect the vacuum.

Eight tanks were used to store the gases, three for the pure component and five for methane-ethane mixtures. They were connected in parallel to form a feed-supply system. The system could be evacuated and flushed with feed alternately before feeding.

The hydrocarbon mixture or the heavier component was first introduced into the equilibrium cell and liquified, then followed by nitrogen. The nitrogen was introduced through a preasure regulator.

Material

Research grade gases supplied by the Matheson of Canada, Ltd., were used in the investigation without any further purification. Specified minimum purities of these gases were as follows:

Nitrogen	99.999	mole %
Methane	99.99	mole %
Ethane	99.9	mole %

Experimental Procedure

After the bath was cooled to the required temperature, hydrocarbon gases were charged. The return line from the volume regulator was closed and nitrogen was allowed to bubble as slowly as possible through the liquid hydrocarbons. As soon as the desired pressure was reached, the pump was switched on for circulation for 10 to 20 minutes, then the charging valve was closed and the valve of return line from the volume regulator was opened while the circulation was continued.

After two or more hours of operation, the circulation was stopped for a short while and the temperature and pressure were recorded. The circulation was resumed, the sample was then taken and analyzed for composition.

When there were two liquid phases in equilibrium with the vapour, the liquid phases were allowed to settle for more than one hour before reading the temperature, the pressure and before any samples were withdrawn from the equilibrium cell.

Analytical Method

After the system reached equilibrium and temperature and pressure were recorded, the vapour sample was trapped in the vapour sampling tube. A portion of liquid in the cell was withdrawn through the liquid sampling tubing. Three liquid sampling tubings were extended into the equilibrium cell through a cooling chamber to the different positions, the top, the middle and the bottom of the cell. The different levels of liquid can be taken by different tubes.

The liquid sampling tubes were installed through the vapour outlet chamber to maintain them at the bath temperature. Furthermore, a needle valve and a three-way valve were installed in between the liquid sampling tube and the sampling bulbs. The sampling bulbs were of 10 ml capacity.

The vapour and liquid sample were analyzed by a Fisher gas partitioner Model 25 V along with Disc Chart integrator Model 232.

Helium gas was used as the carrier gas which swept the sample through two chromatographic columns connected in series, with a detector at the end of each column. The two columns had different dimensions and were packed with different materials.

In this study, no packing material was used for column 1 which was 6 inches long by 0.26 inch OD. Column two was 6 1/2 feet long by 0.25 inch OD, filled with 28-30 mesh silica gel. The helium flow rate through the gas partitioner was 85 c.c. per minute at pressure of 20 psig. The column temperature was 40°C. The chart speed of the recorder was 1/2 inch per minute. A retention time of 6 to 8 minutes was required for separating the three components. A typical analysis is shown in Fig. 3.

The calibration curves for the binary mixture are shown in Appendix III.

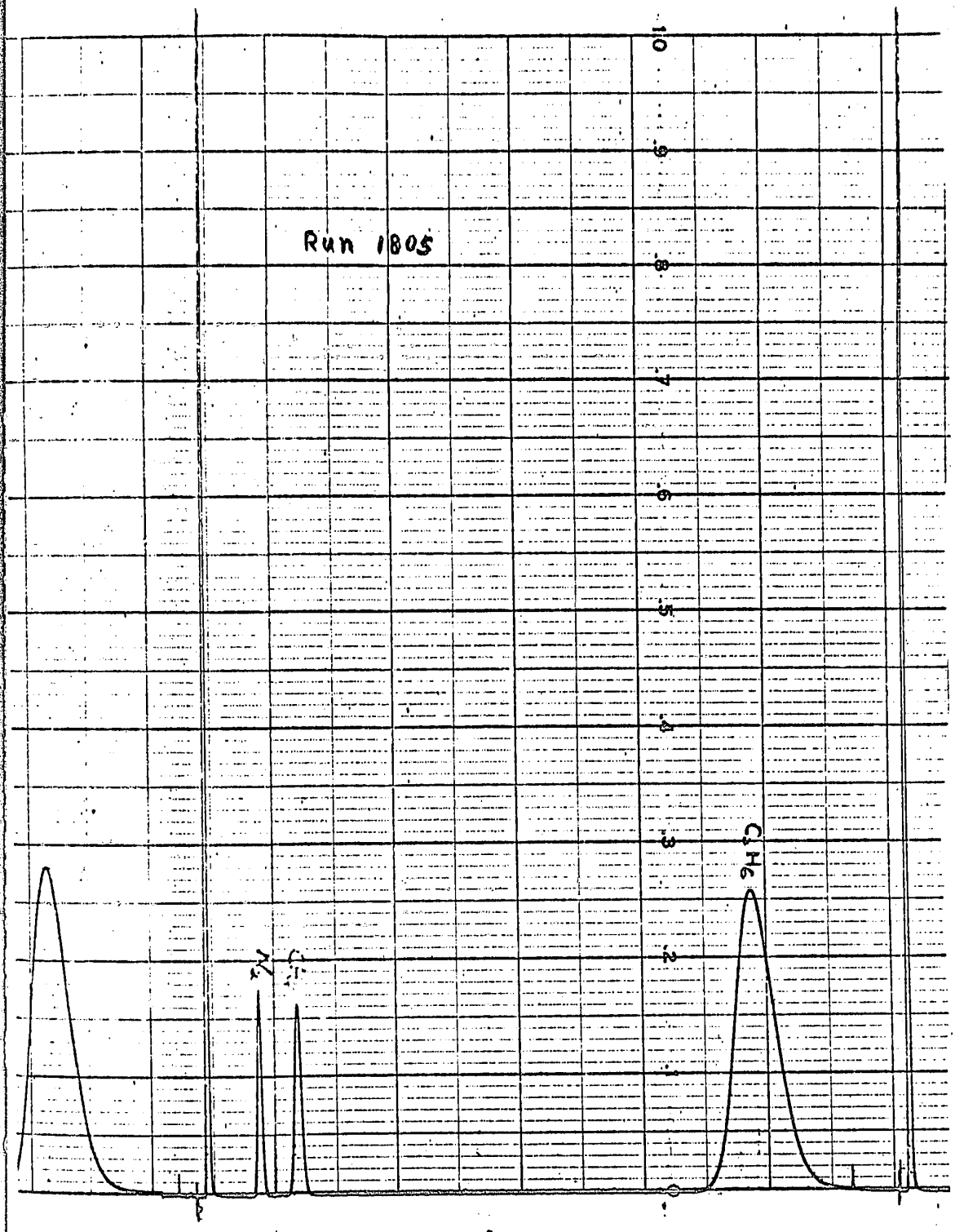

Figure 3. Chromatogram of run 1805

RESULTS AND CORRELATION OF DATA

The experimental equilibrium temperature-pressure-composition data obtained for the binary nitrogen-methane and nitrogen-ethane systems are listed in Tables I and II. Smoothed data for these systems are listed in Tables III and IV. Experimental vapour-liquid data for the ternary system nitrogen-methane-ethane are listed in Table V. K values for ternary system nitrogen-methane-ethane are listed in Table VI. Experimental liquid-liquid-vapour equilibrium data for the nitrogen-ethane binary, and the ternary system nitrogen-methane-ethane are listed in Table VII.

Isothermal pressure-composition plots for binary systems nitrogen-methane and nitrogen-ethane are shown in Figures 4 to 7.

Vapourization constant, K, were correlated as a function of pressure for binary systems nitrogen-methane and nitrogen-ethane. The correlations are shown in Figures 8 and 9.

Isothermal vapour-liquid compositions for the ternary system nitrogen-methane-ethane are shown in Figures 10 to 14.

K-values for the compositions in the ternary system nitrogen-methane-ethane were correlated as a function of pressure and composition at -225.5°F. The correlations are shown in Figure 15, using $x_{CH_4}/(x_{CH_4} + x_{C_2H_6})$ as the parameter.

Experimental liquid-liquid-vapour equilibrium data for the ternary nitrogen-methane-ethane are shown in Figure 16 to 18. Temperature-composition plots for binary system nitrogen-ethane in three coexisting phases are shown in Figure 19.

Liquid-liquid-vapour equilibrium compositions were correlated in terms of distribution coefficients, K'_i, and solubility function K'_H. These correlations are shown in Figures 20 to 22. From Figures 20 to 22, change of K'_H values with temperature at constant K'_i values were obtained. They were plotted in Figures 23 to 25.

For liquid-liquid-vapour equilibrium data vapourization constant, K were correlated as a function of pressure for the ternary system nitrogen-methane-ethane. The correlations are shown in Figures 26 and 27. As concentration of the ethane is extremely low in the vapour phase, any small variation of the ethane concentration in vapour phase composition would affect considerably the K_{C_2} values. For this reason, no correlation was made for K_{C_2}.

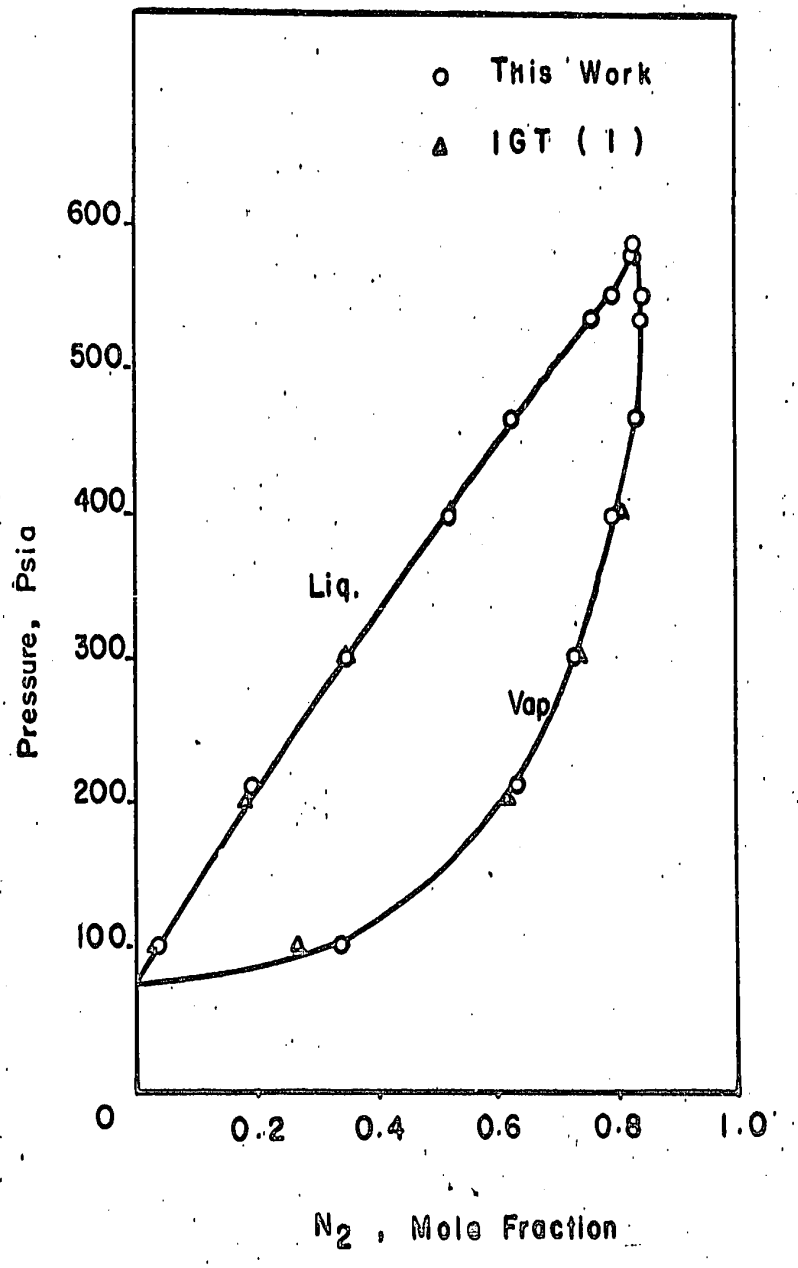

Figure 4. The p-x-y diagram of the nitrogen-methane system at -216.3°F.

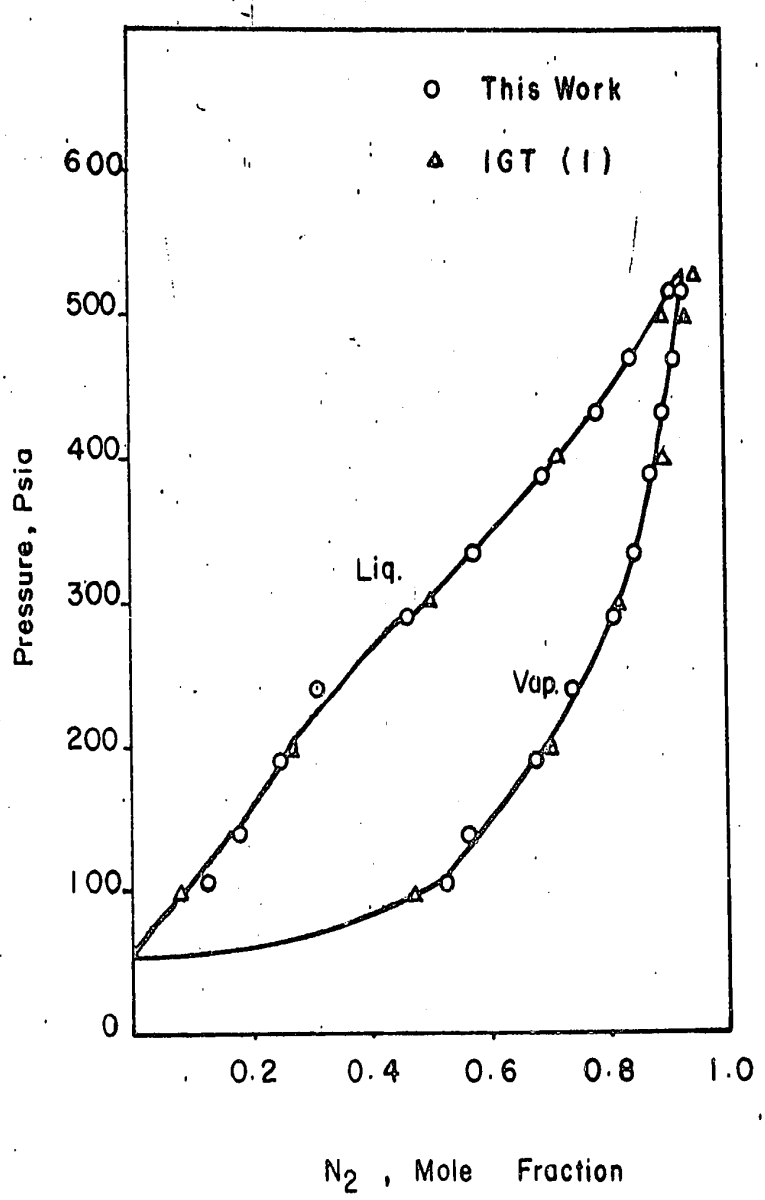

Figure 5. The p-x-y diagram of the nitrogen-methane system at -225.5 °F

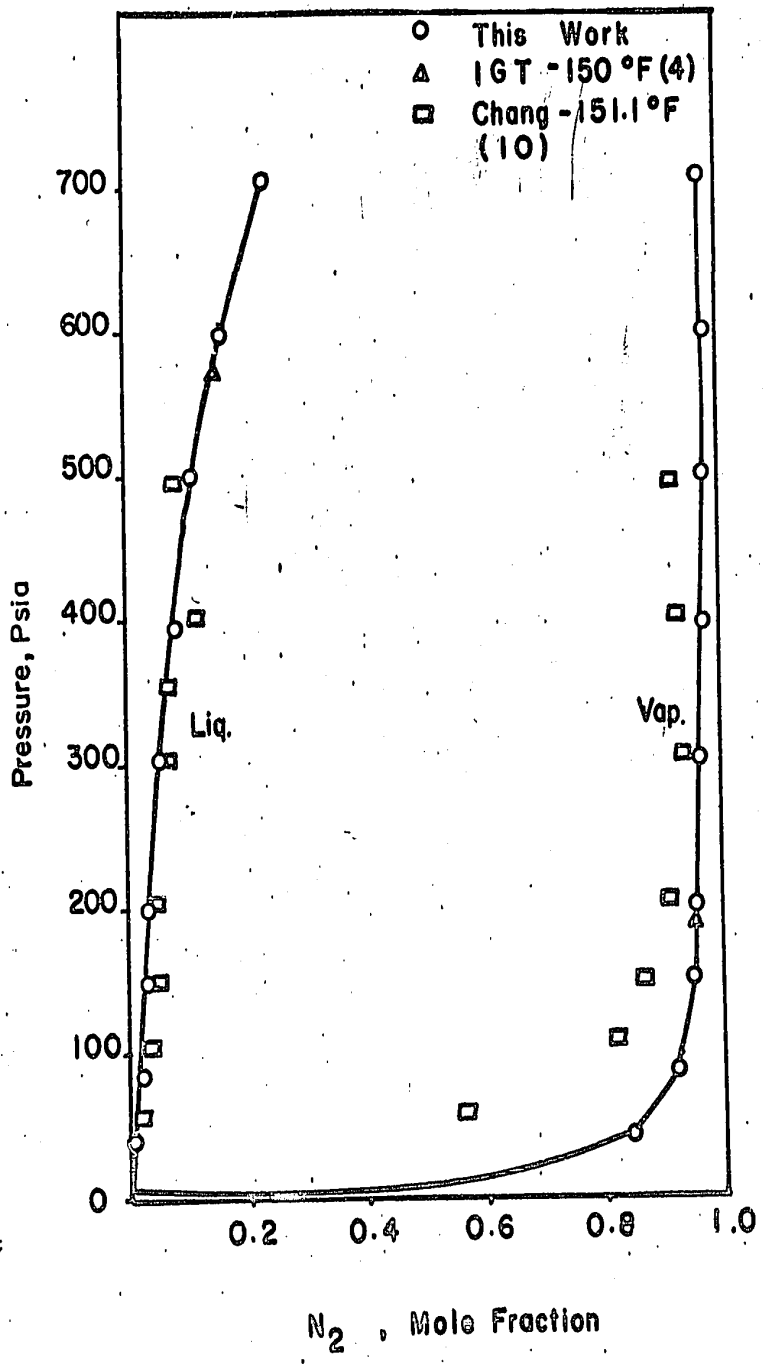

Figure 6. The p-x-y diagram of the nitrogen-ethane system at -153.1°F.

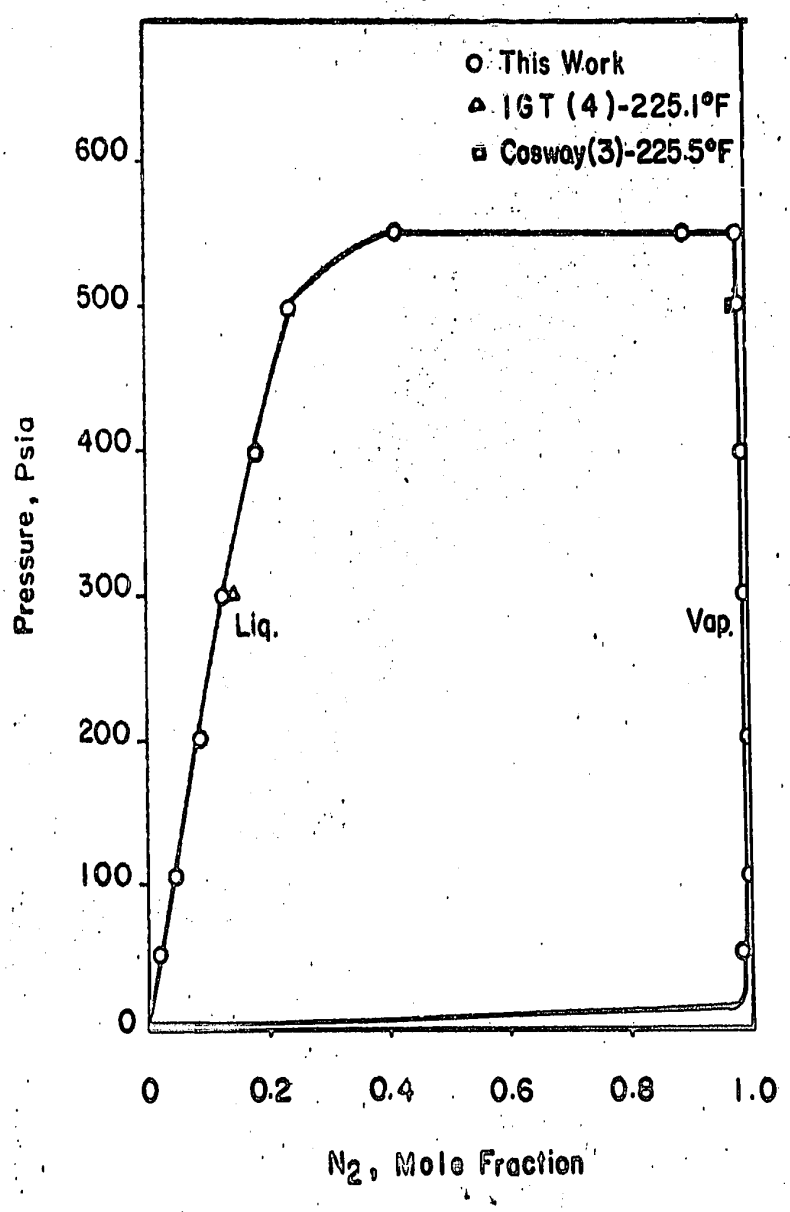

Figure 7. The p-x-y diagram of the nitrogen-ethane system at -225.5°F.

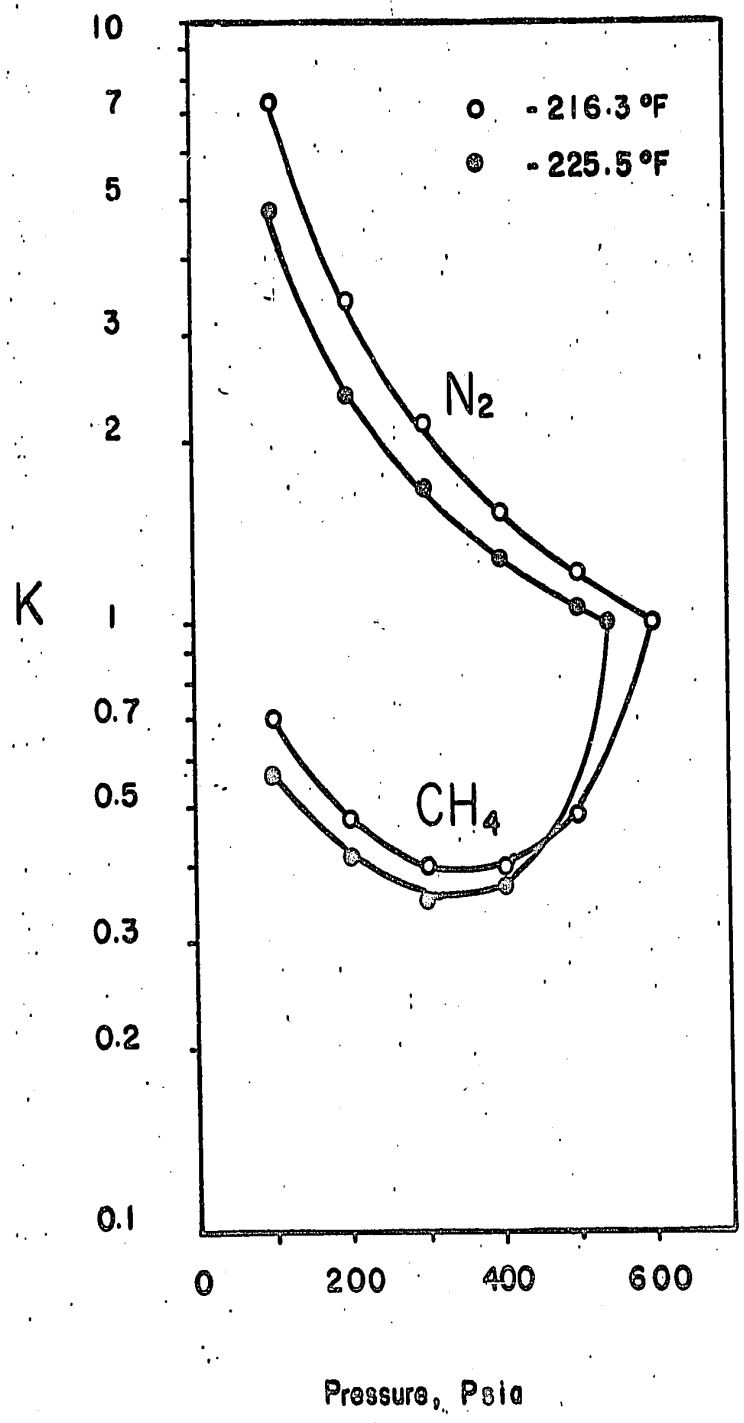

Figure 8. The K-P diagram of the nitrogen-methane system.

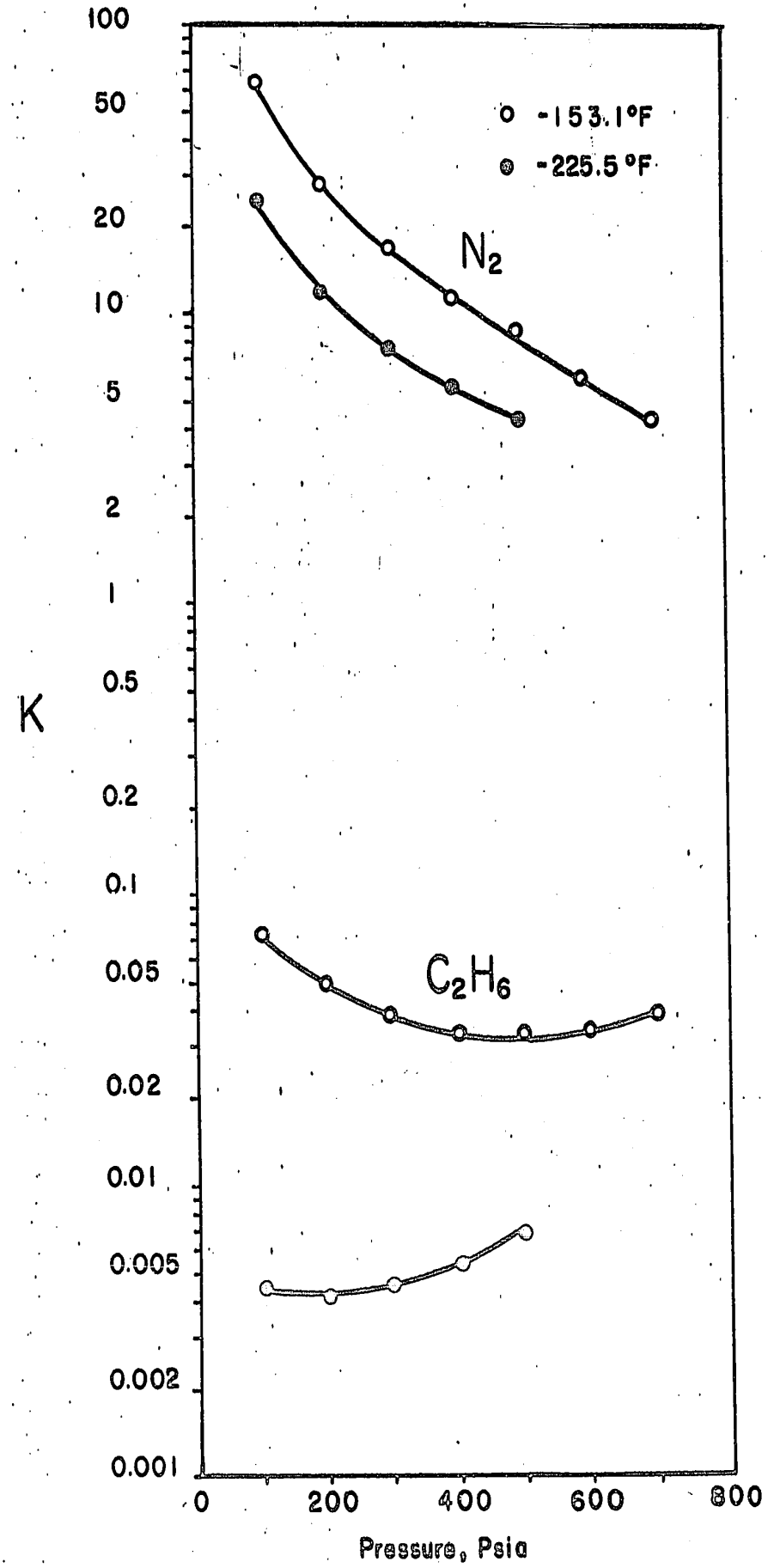

Figure 9. The K-P diagram of the nitrogen-ethane system.

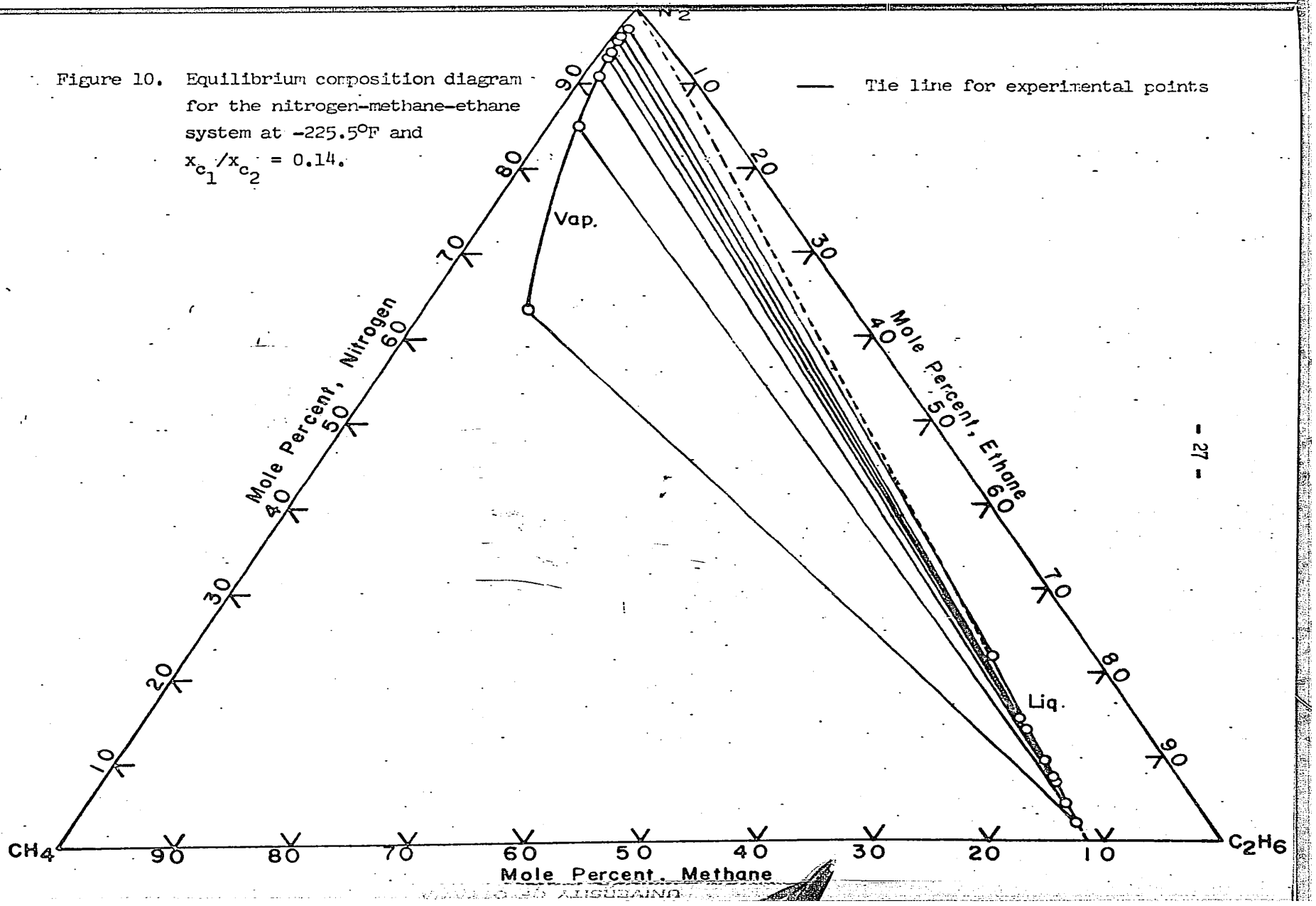

Figure 10. Equilibrium composition diagram for the nitrogen-methane-ethane system at -225.5°F and $x_{c_1}/x_{c_2} = 0.14$.

—— Tie line for experimental points

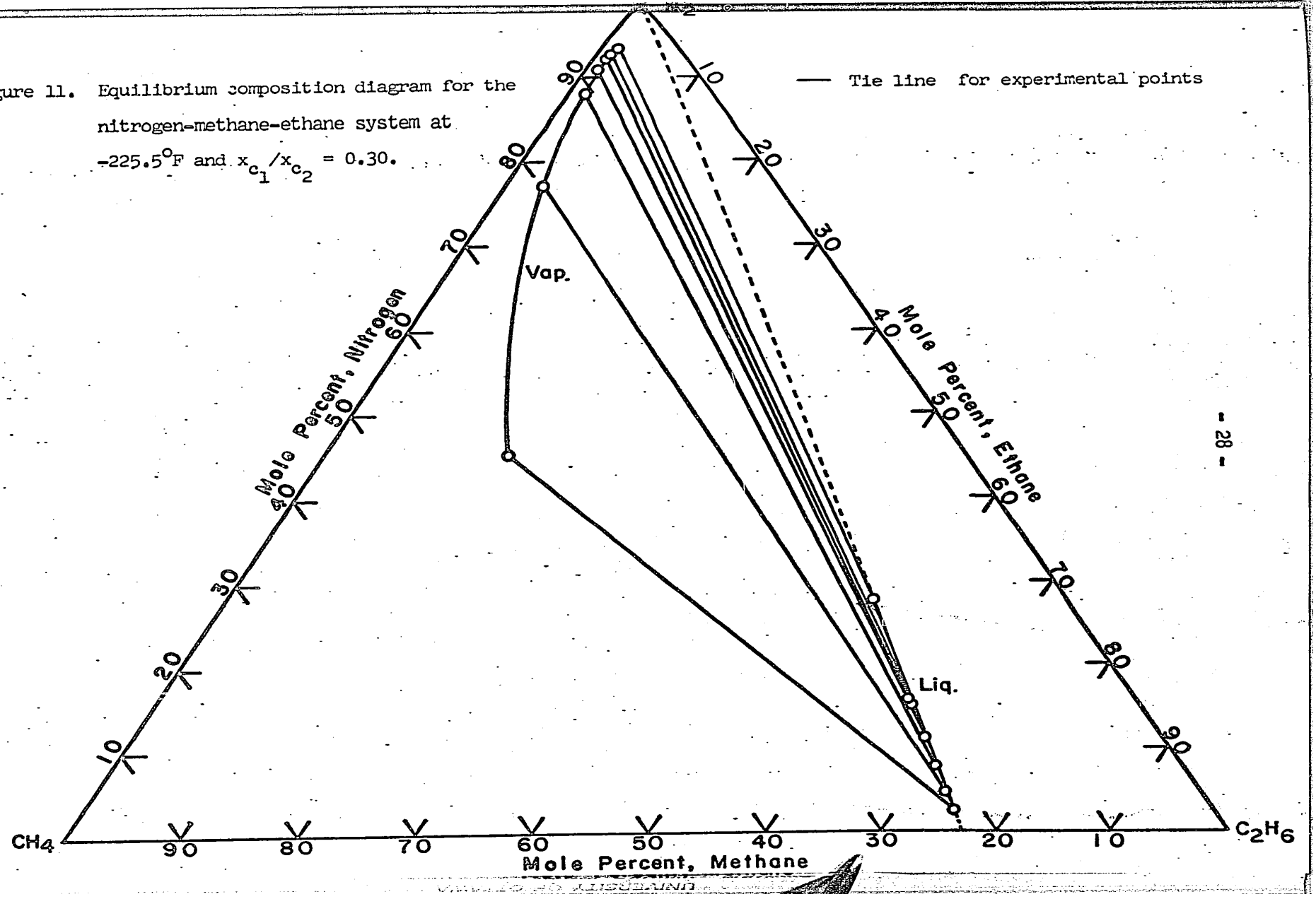

Figure 11. Equilibrium composition diagram for the nitrogen-methane-ethane system at $-225.5^{\circ}F$ and $x_{c_1}/x_{c_2} = 0.30$.

—— Tie line for experimental points

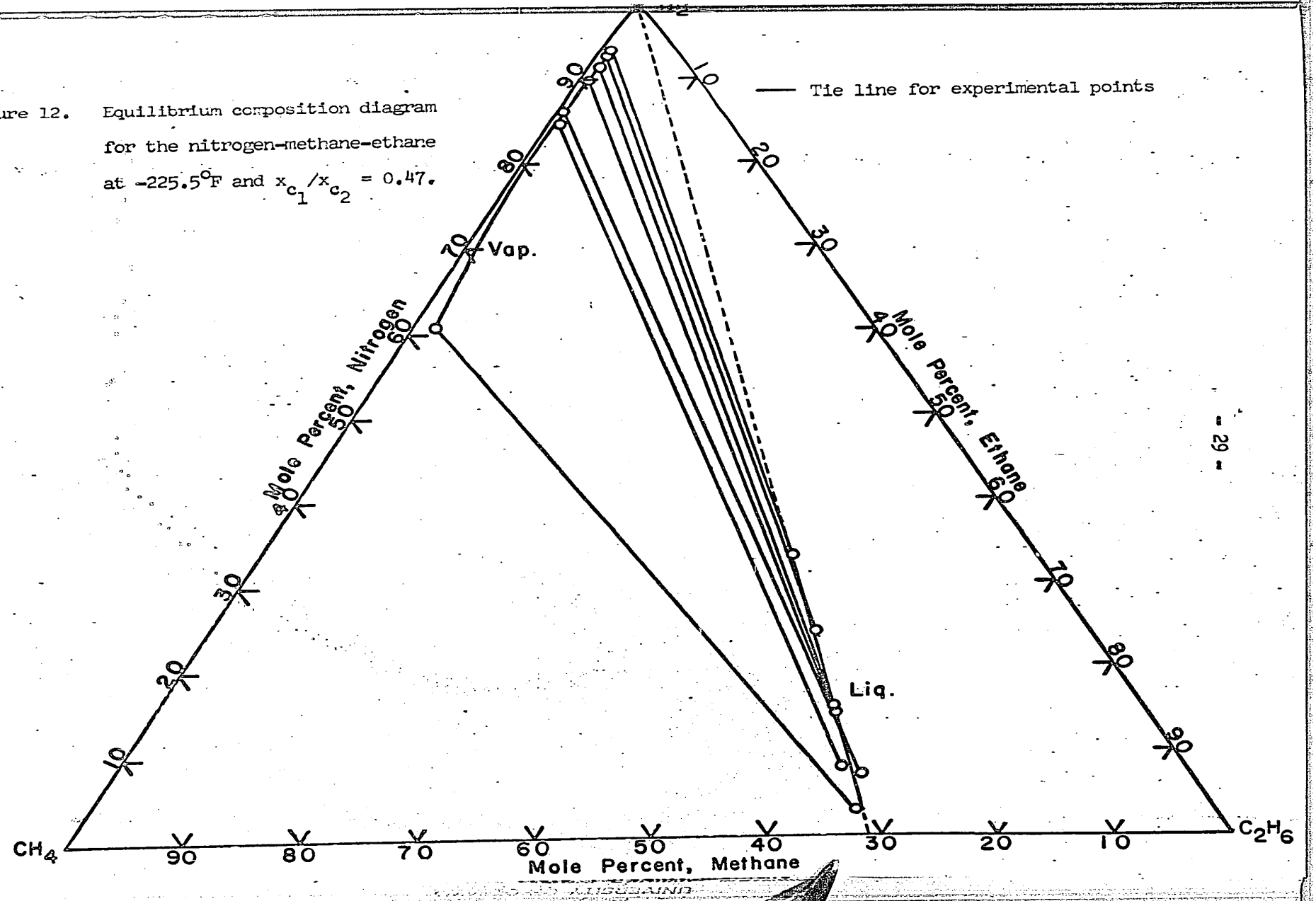

Figure 12. Equilibrium composition diagram for the nitrogen-methane-ethane at -225.5°F and $x_{c_1}/x_{c_2} = 0.47$.

Figure 13. Equilibrium composition diagram for the nitrogen-methane-ethane system at -225.5°F and x_{c_1}/x_{c_2} = 1.27

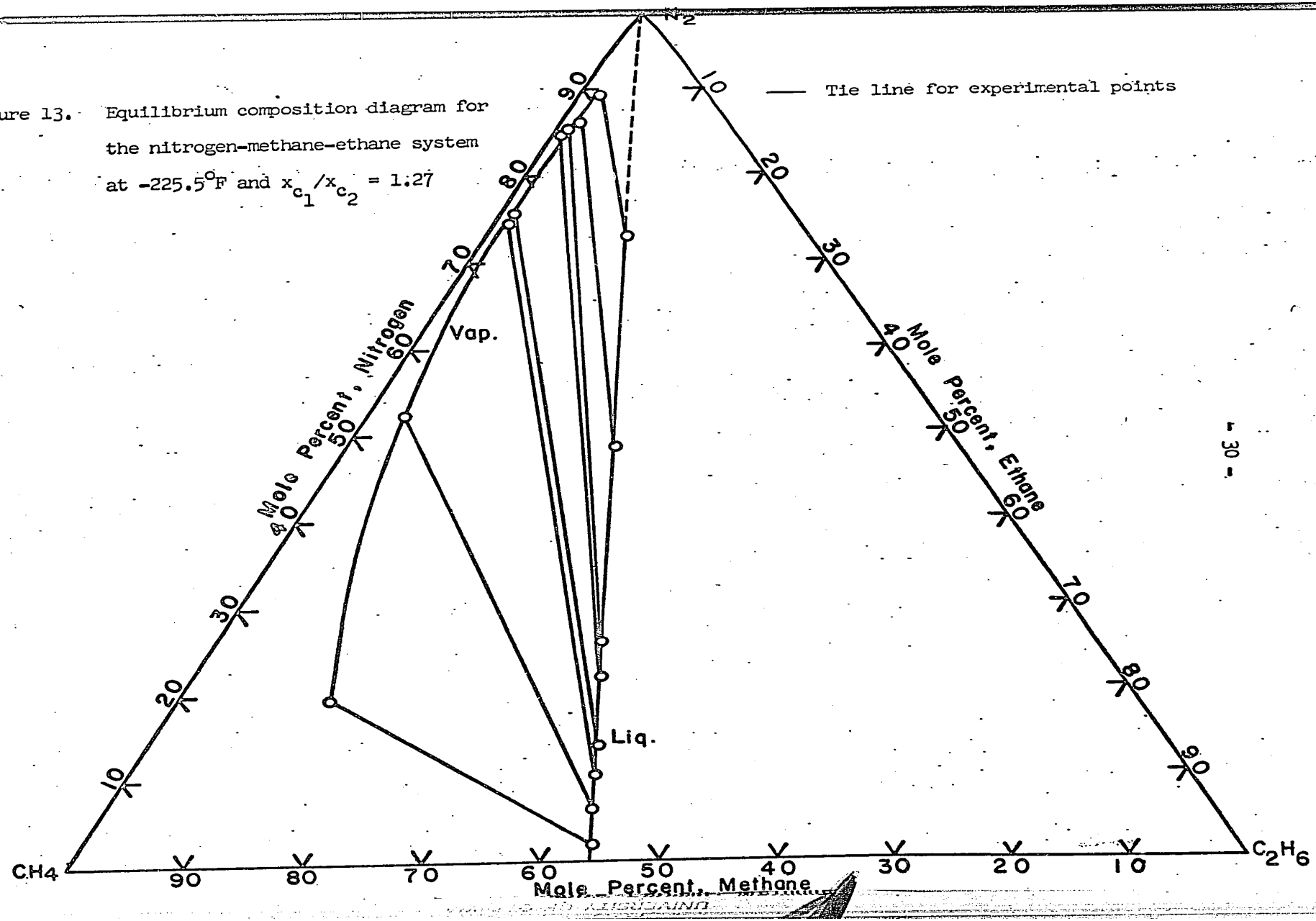

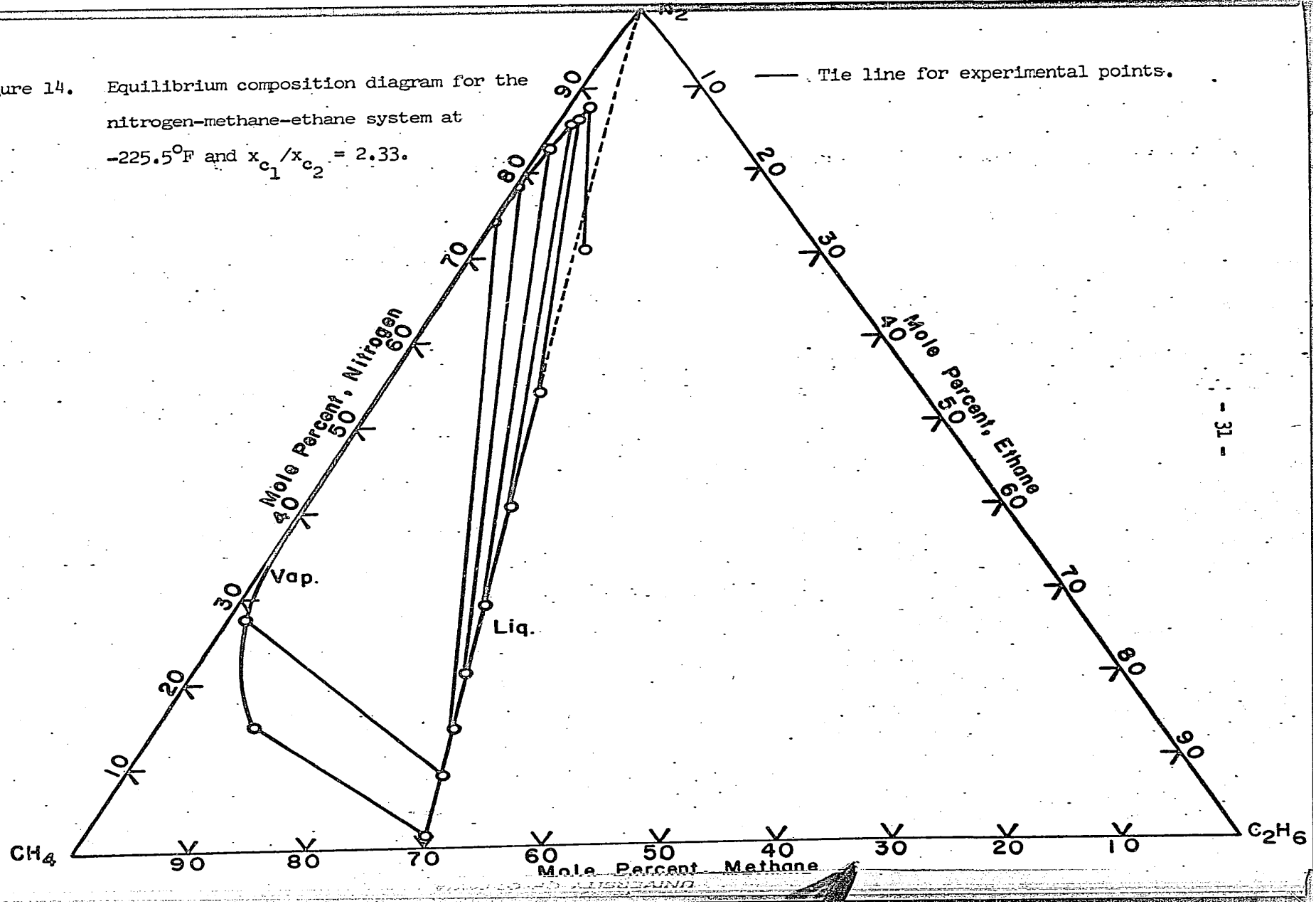

Figure 14. Equilibrium composition diagram for the nitrogen-methane-ethane system at $-225.5^{\circ}F$ and $x_{c_1}/x_{c_2} = 2.33$.

—— Tie line for experimental points.

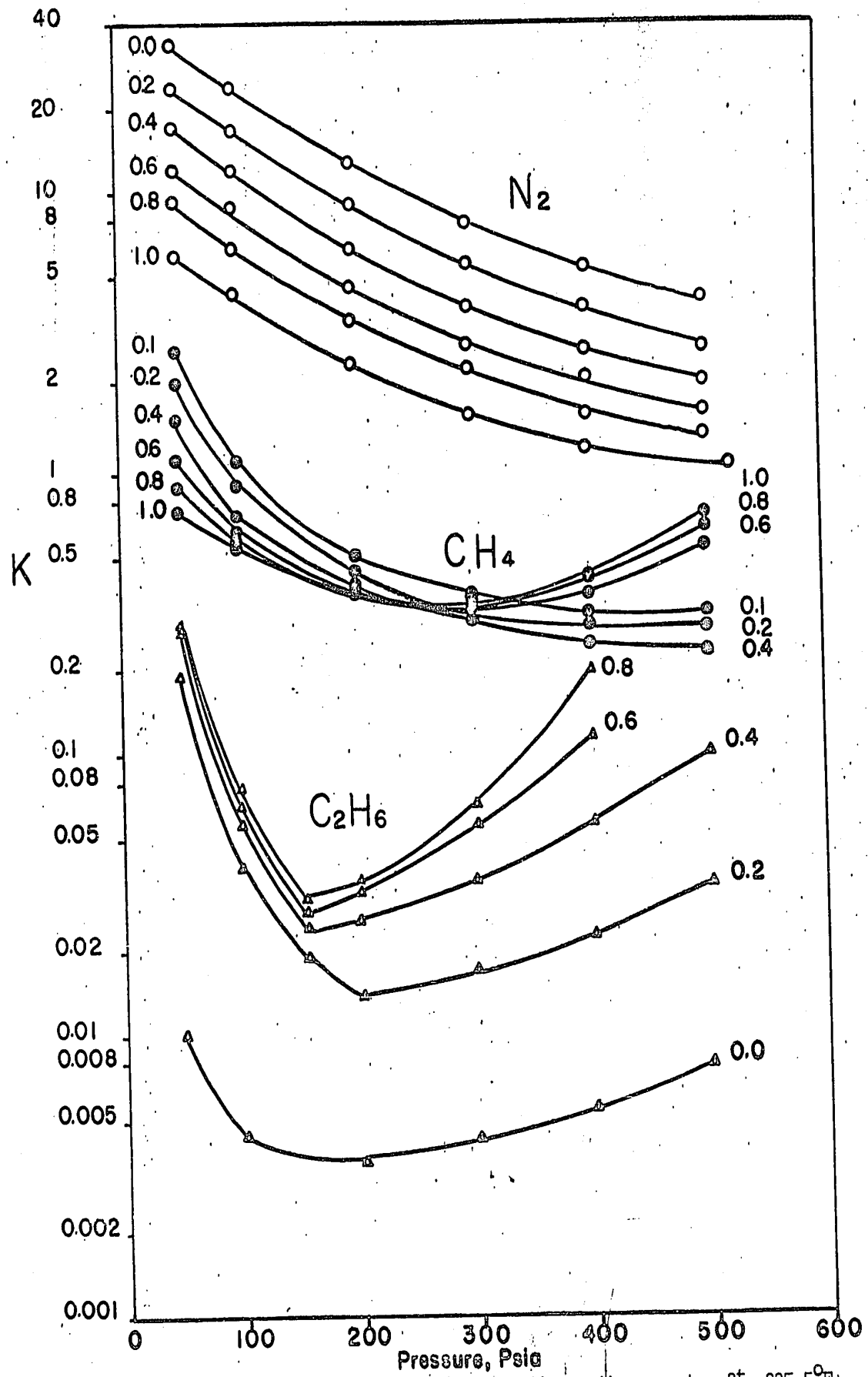

Figure 15. The log K-P diagram for the nitrogen-methane-ethane system at -225.5°F using $x_{c_1}/(x_{c_1} + x_{c_2})$ as parameter.

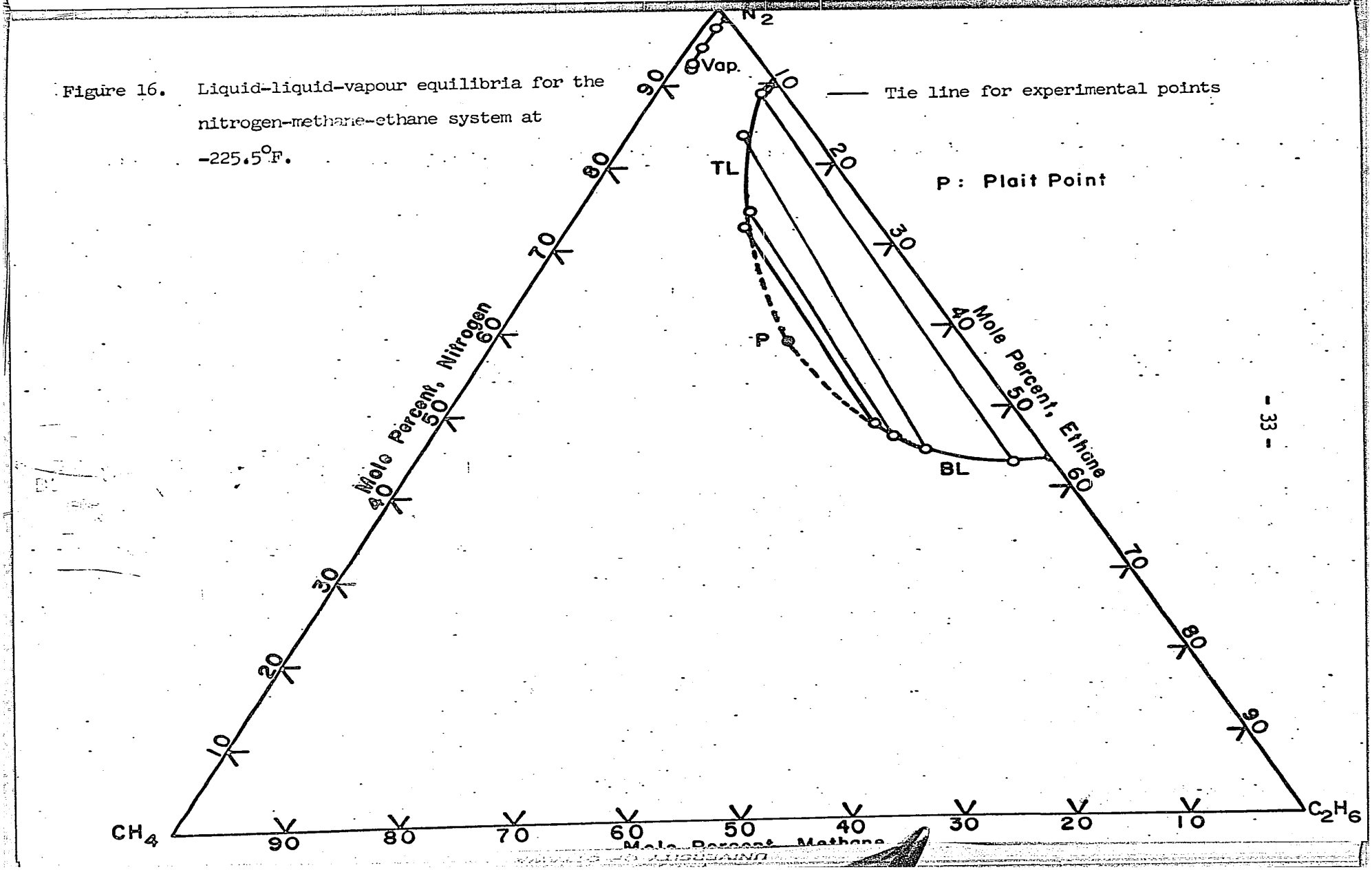

Figure 16. Liquid-liquid-vapour equilibria for the nitrogen-methane-ethane system at -225.5°F.

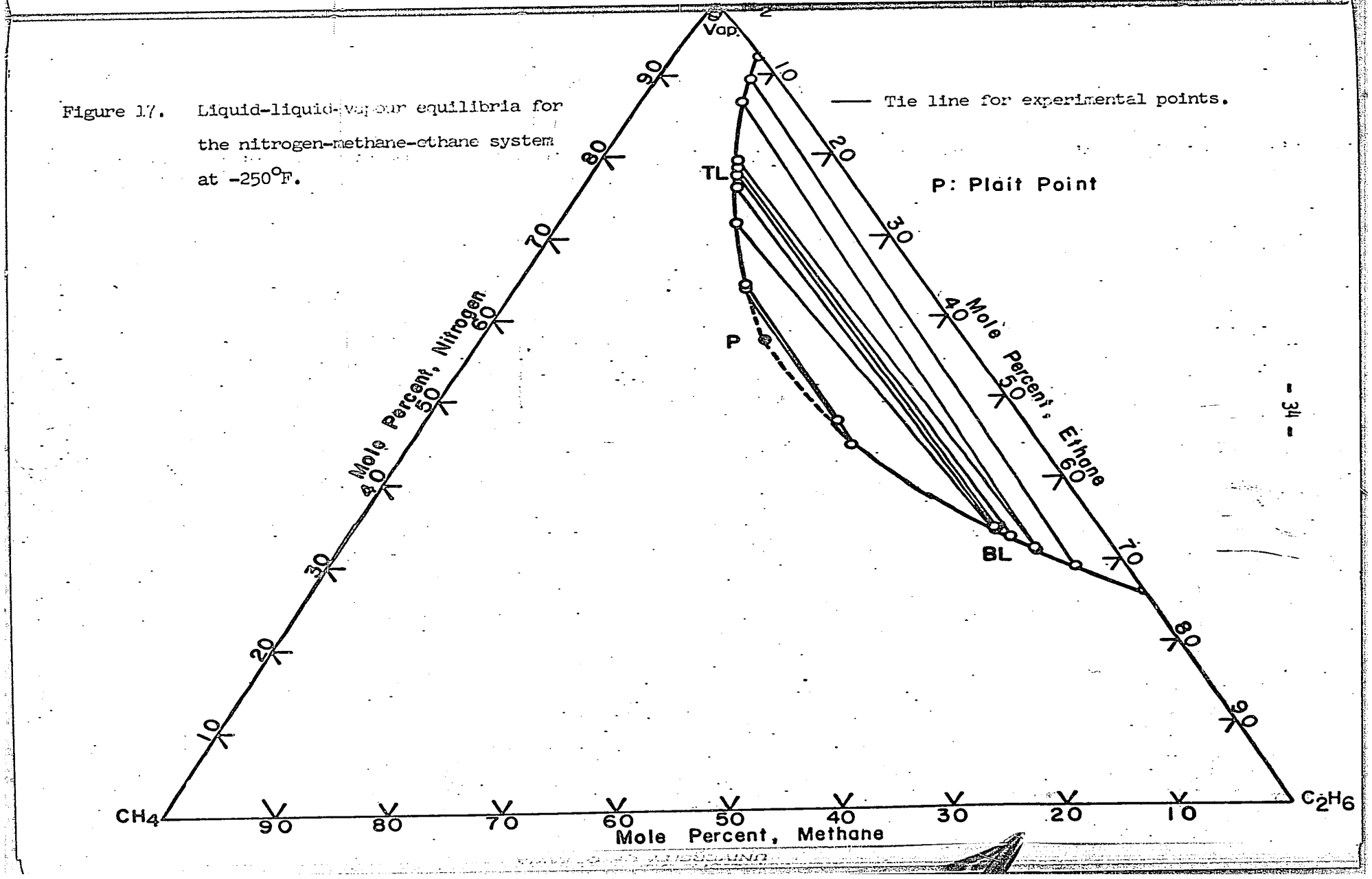

Figure 17. Liquid-liquid-vapour equilibria for the nitrogen-methane-ethane system at -250°F.

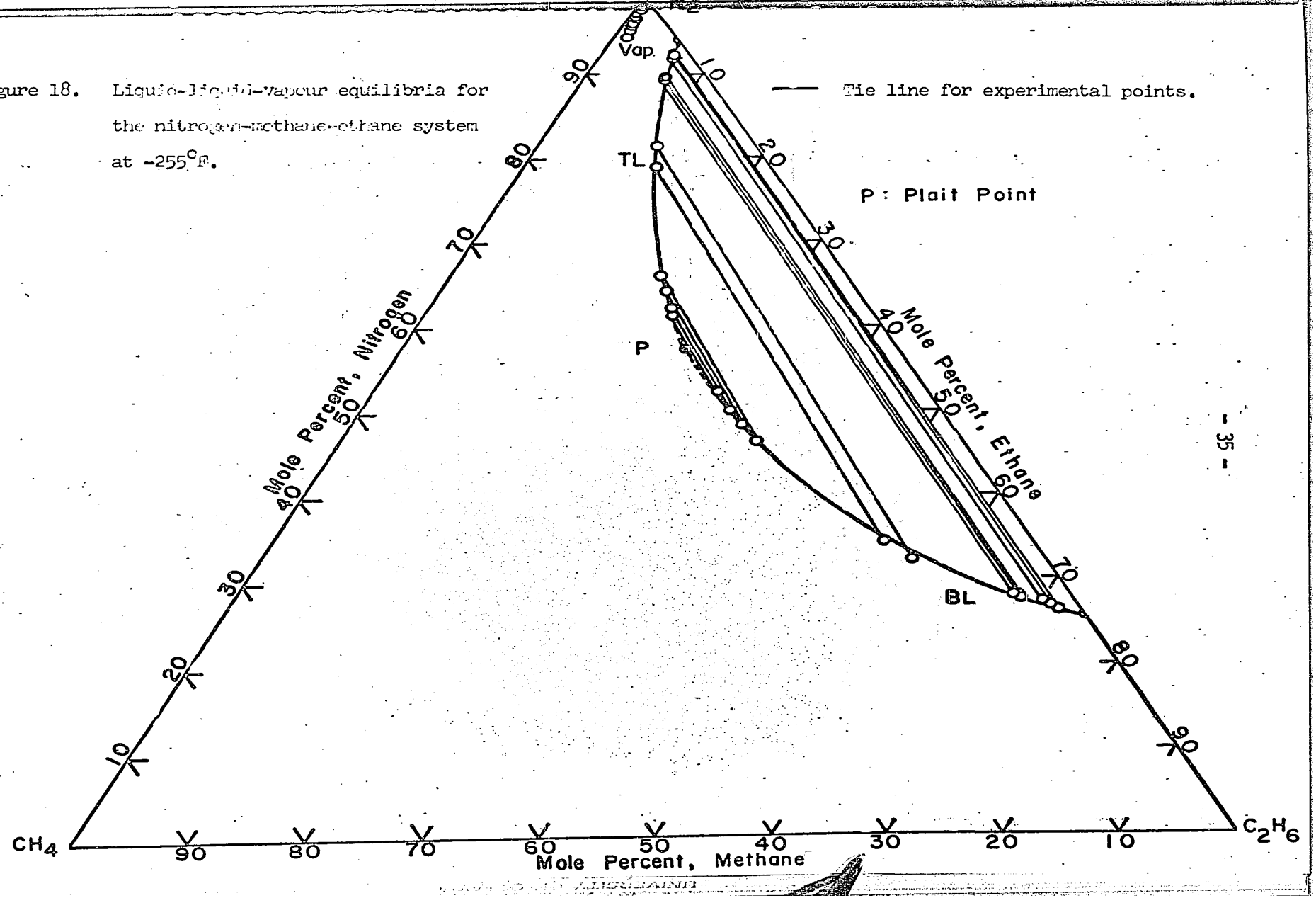

Figure 18. Liquid-liquid-vapour equilibria for the nitrogen-methane-ethane system at -255°F.

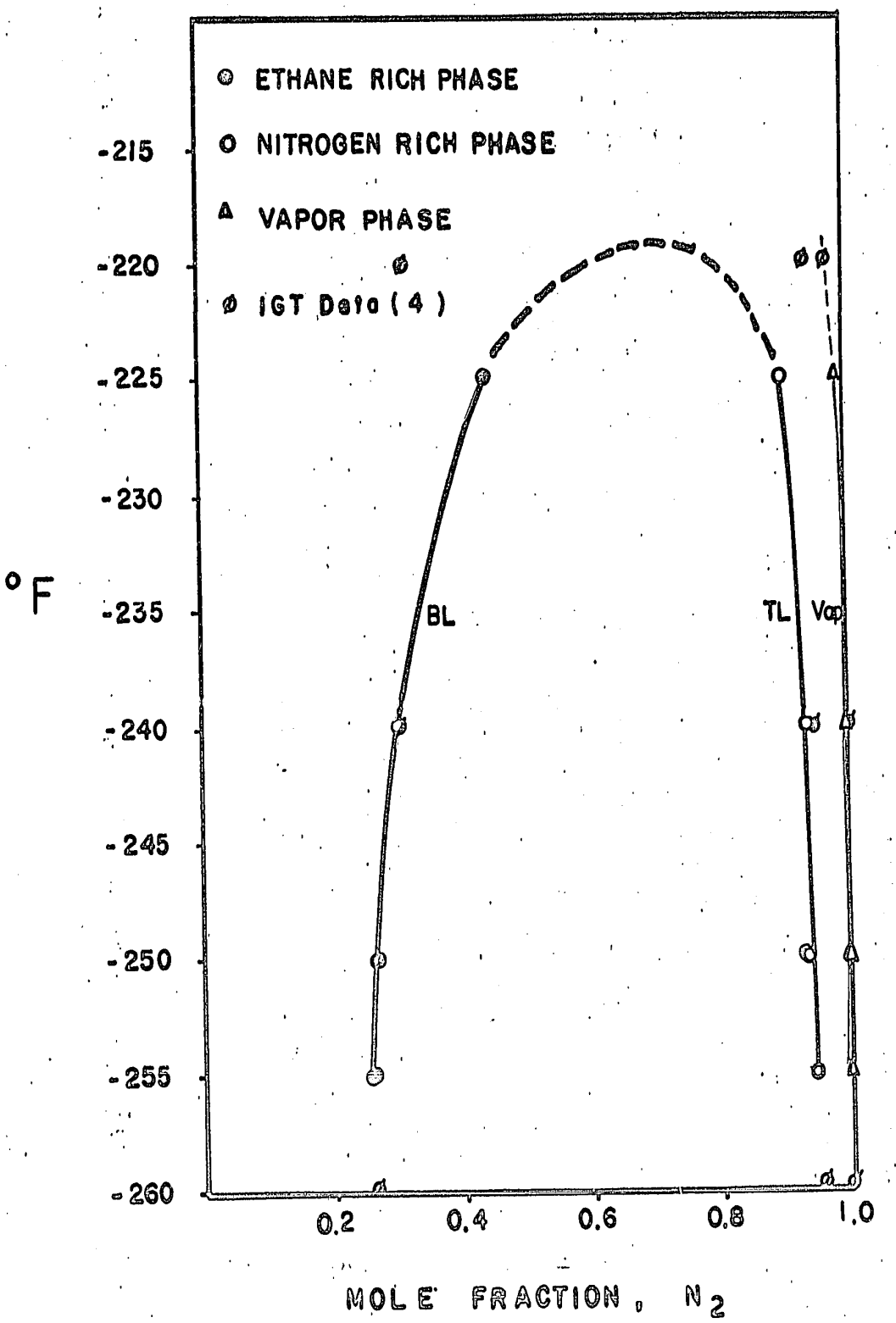

Figure 19. Change of composition of the three co-existing phases with temperature for the nitrogen-ethane system.

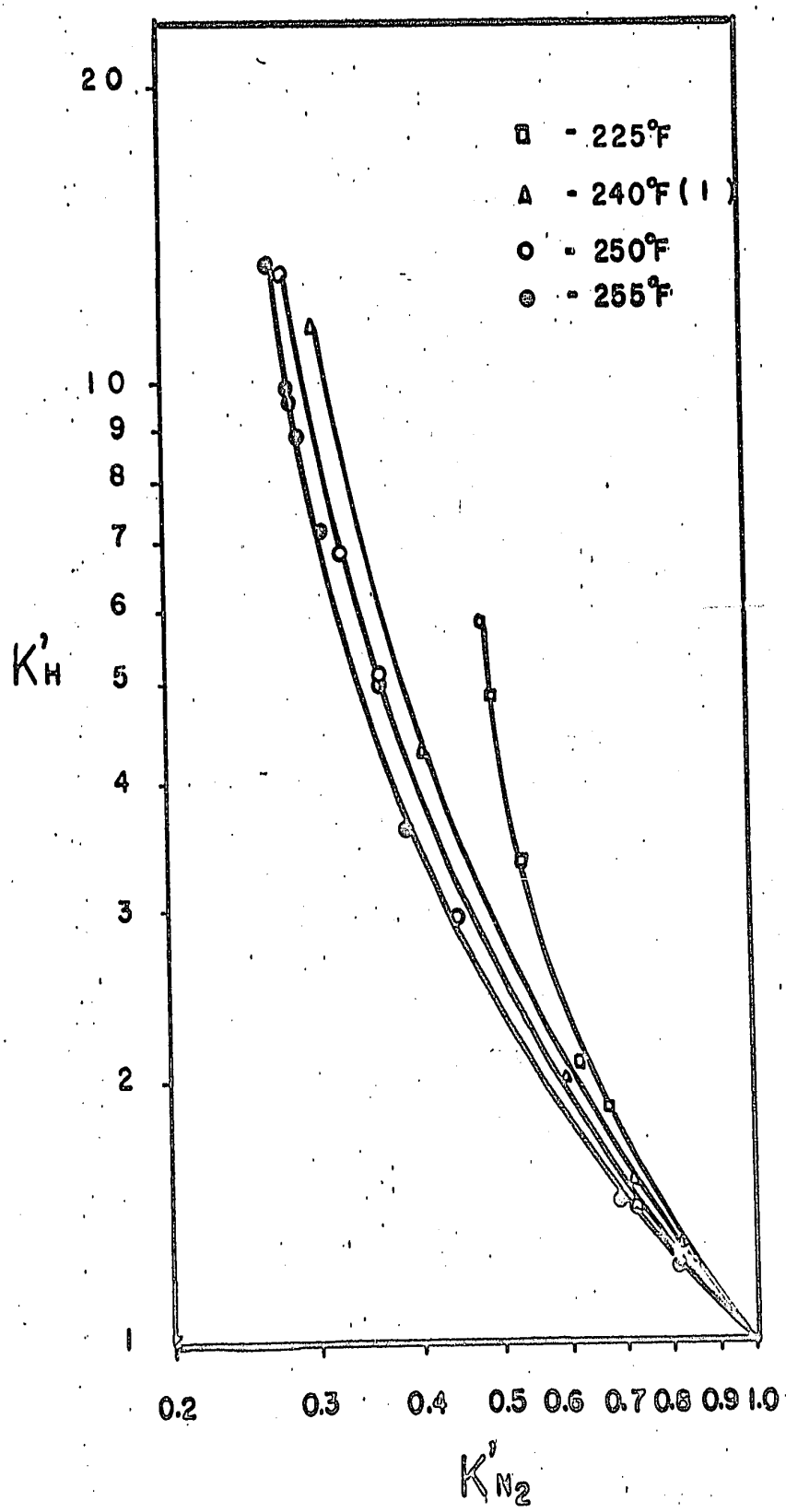

Figure 20. Correlation of the solubility function, K'_H with the liquid-liquid distribution coefficient K'_{N_2}.

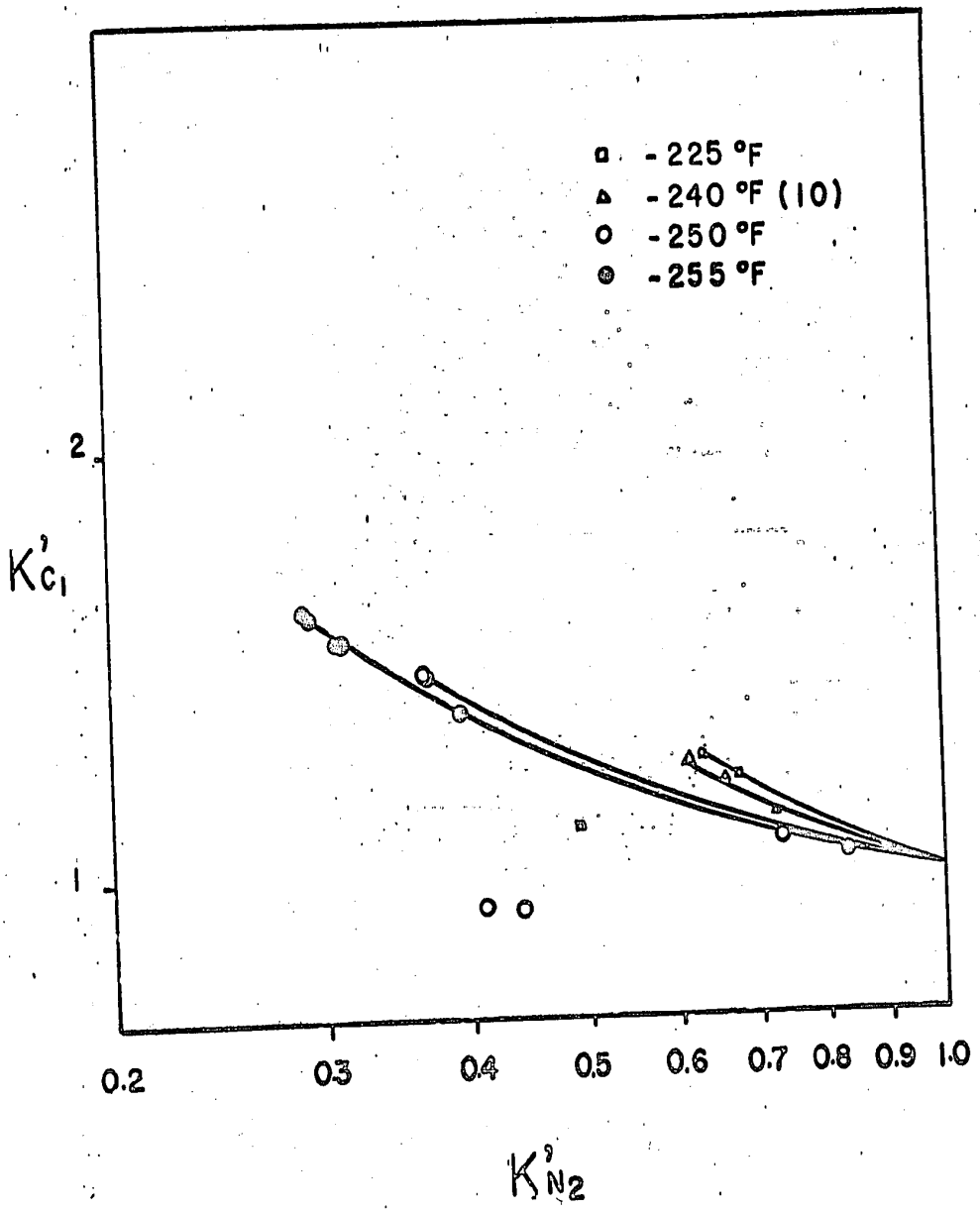

Figure 21. Correlation of the solubility function, K'_{c_1} with the liquid-liquid distribution coefficient K'_{N_2}.

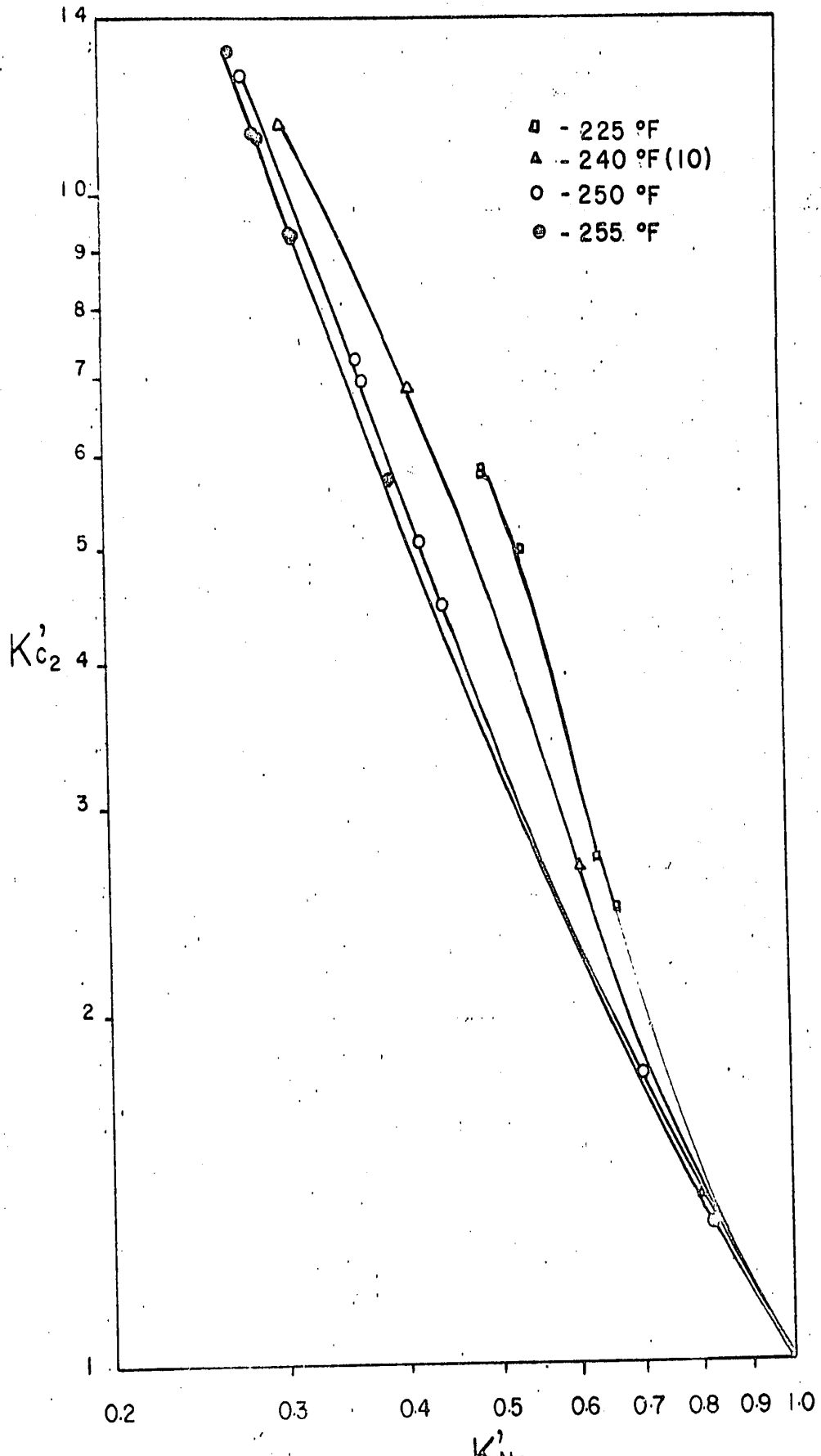

Figure 22. Correlation of the solubility function, $K'_{N_2} K'_{c_2}$ with the liquid-liquid distribution coefficient K'_{N_2}

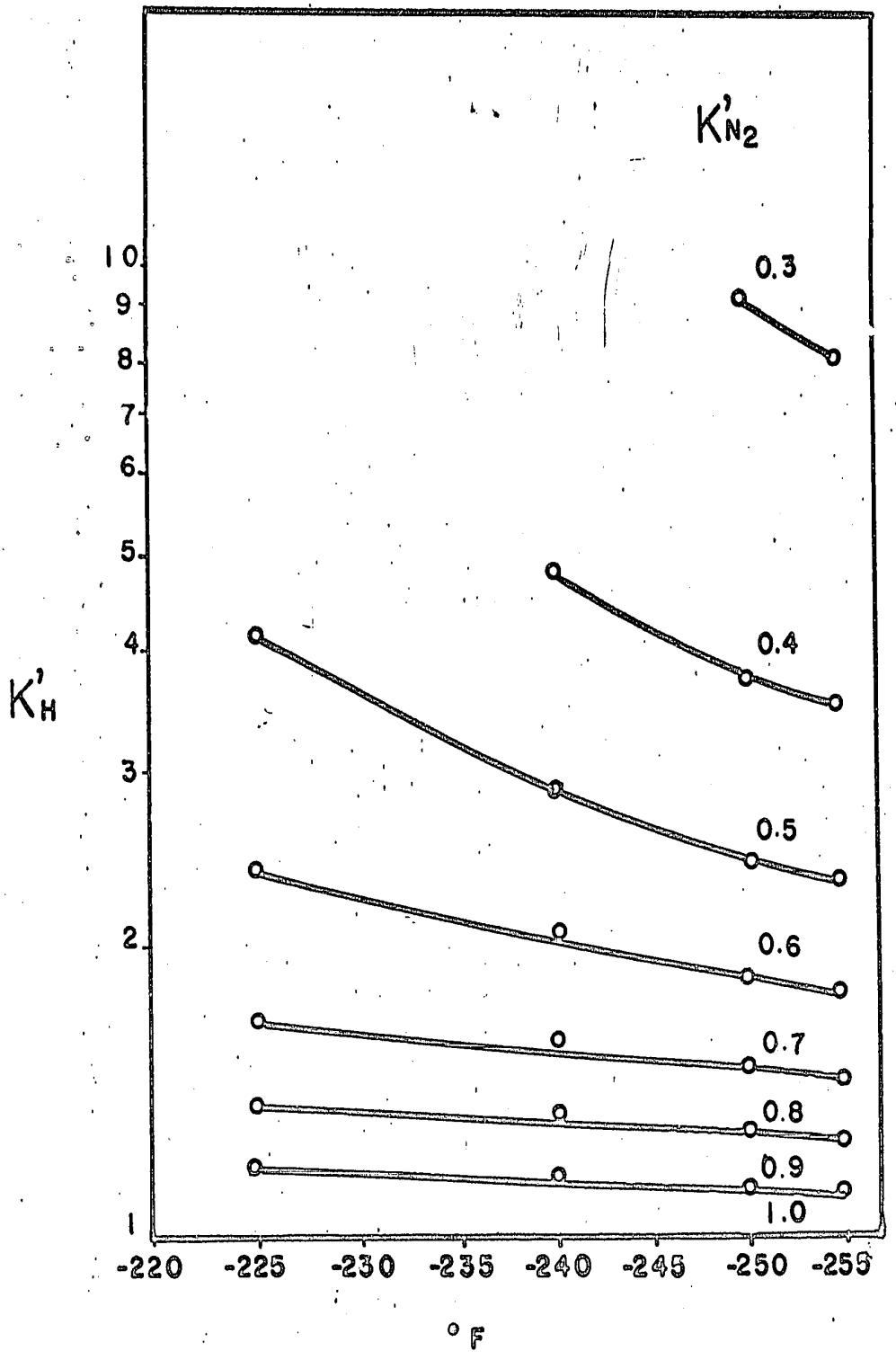

Figure 23. Correlation of the solubility function, K'_H with temperature.

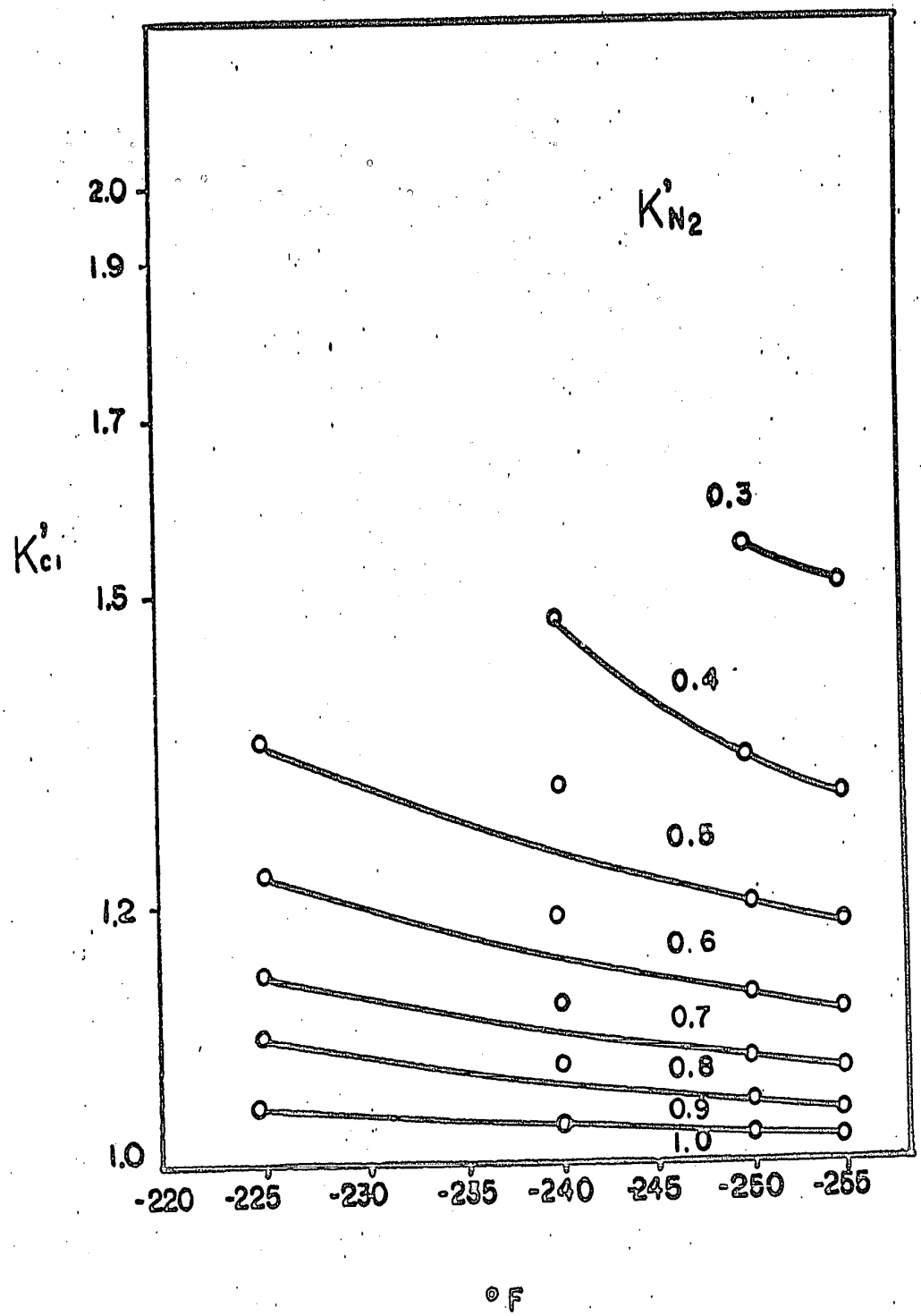

Figure 24. Correlation of the solubility function, K'_{c_1} with temperature.

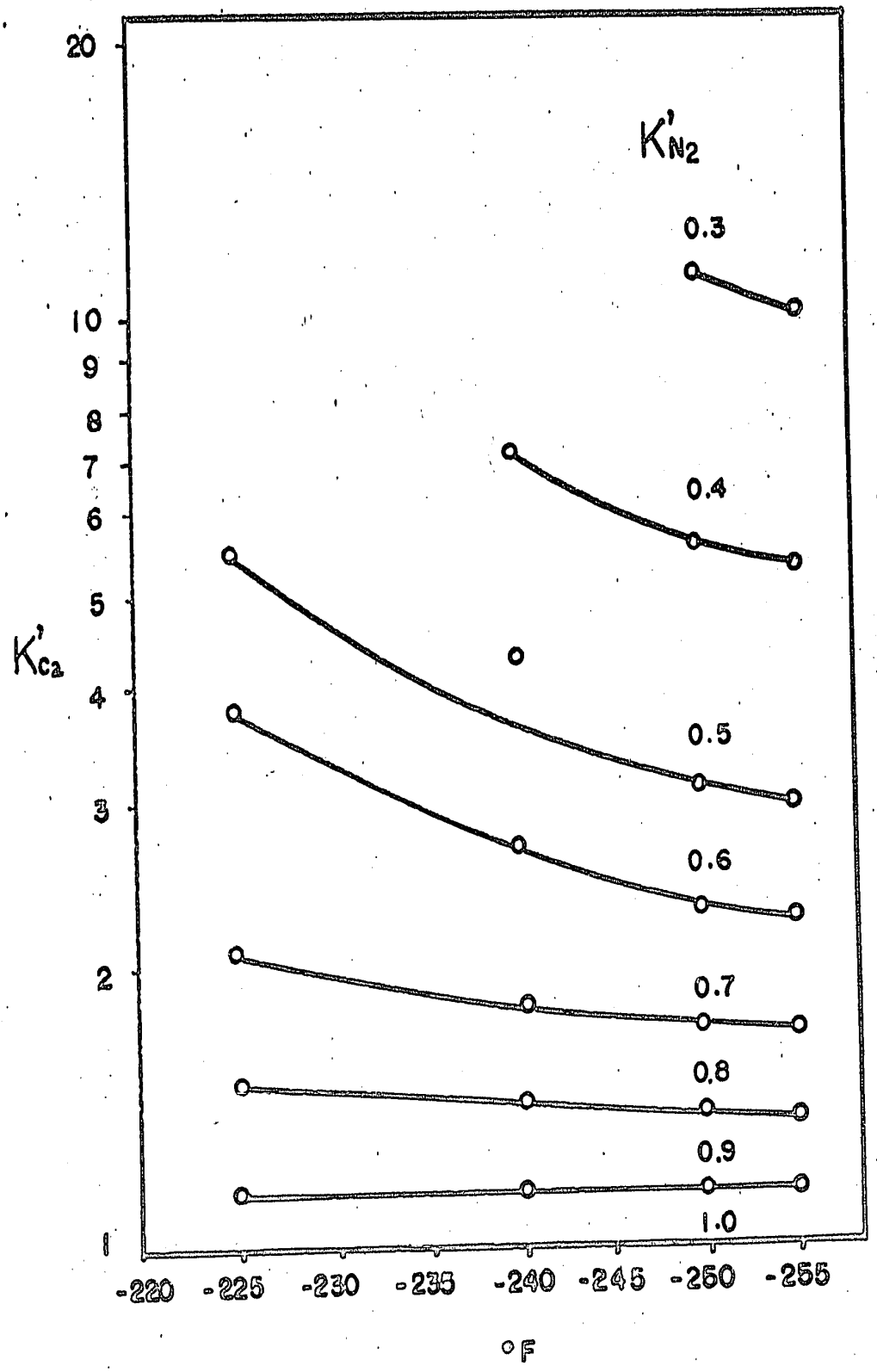

Figure 25. Correlation of the solubility function, K'_{c_2} with temperature.

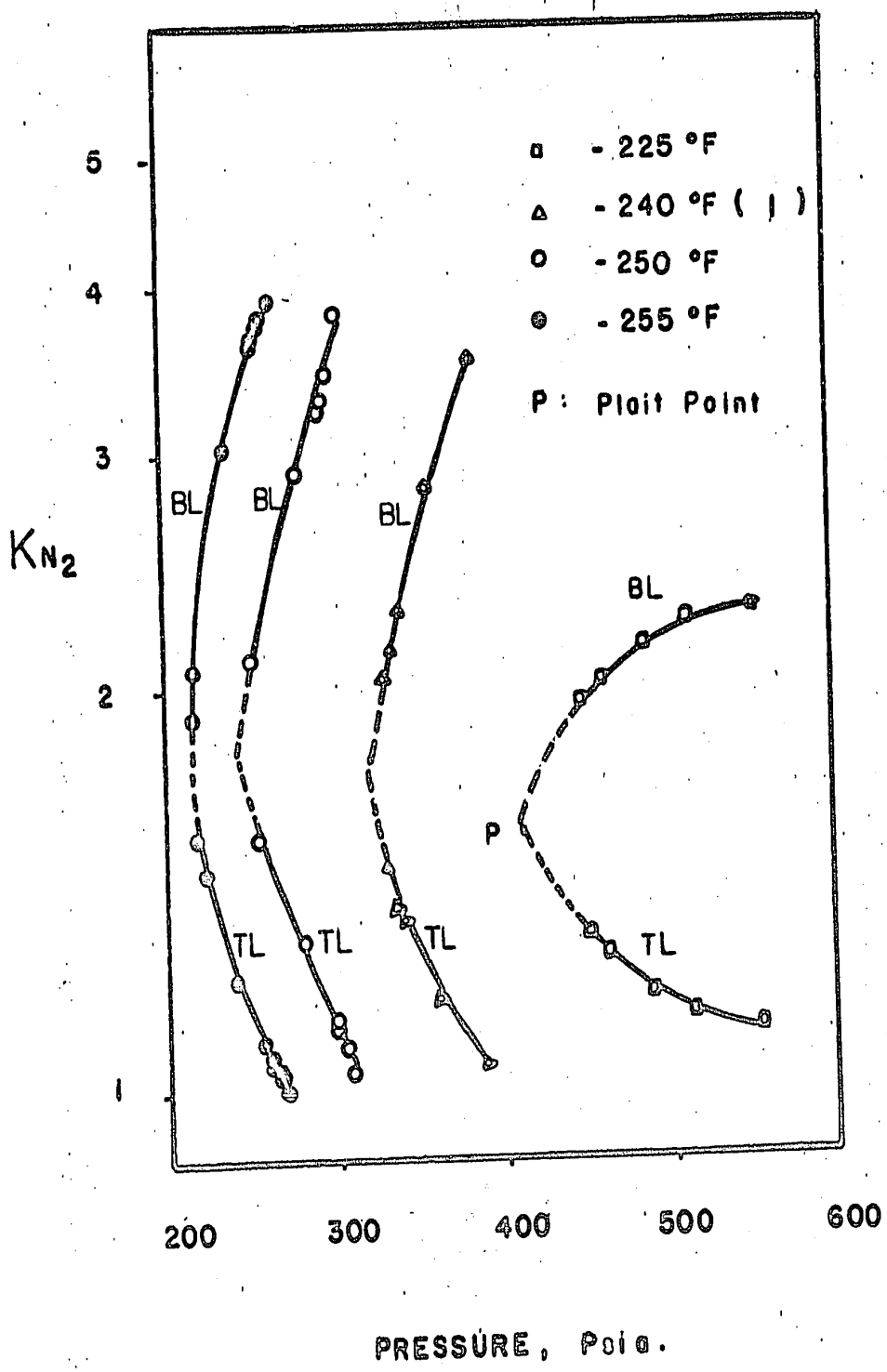

Figure 26. The K_{N_2}-P diagram for the nitrogen-methane-ethane system in the three-phase region.

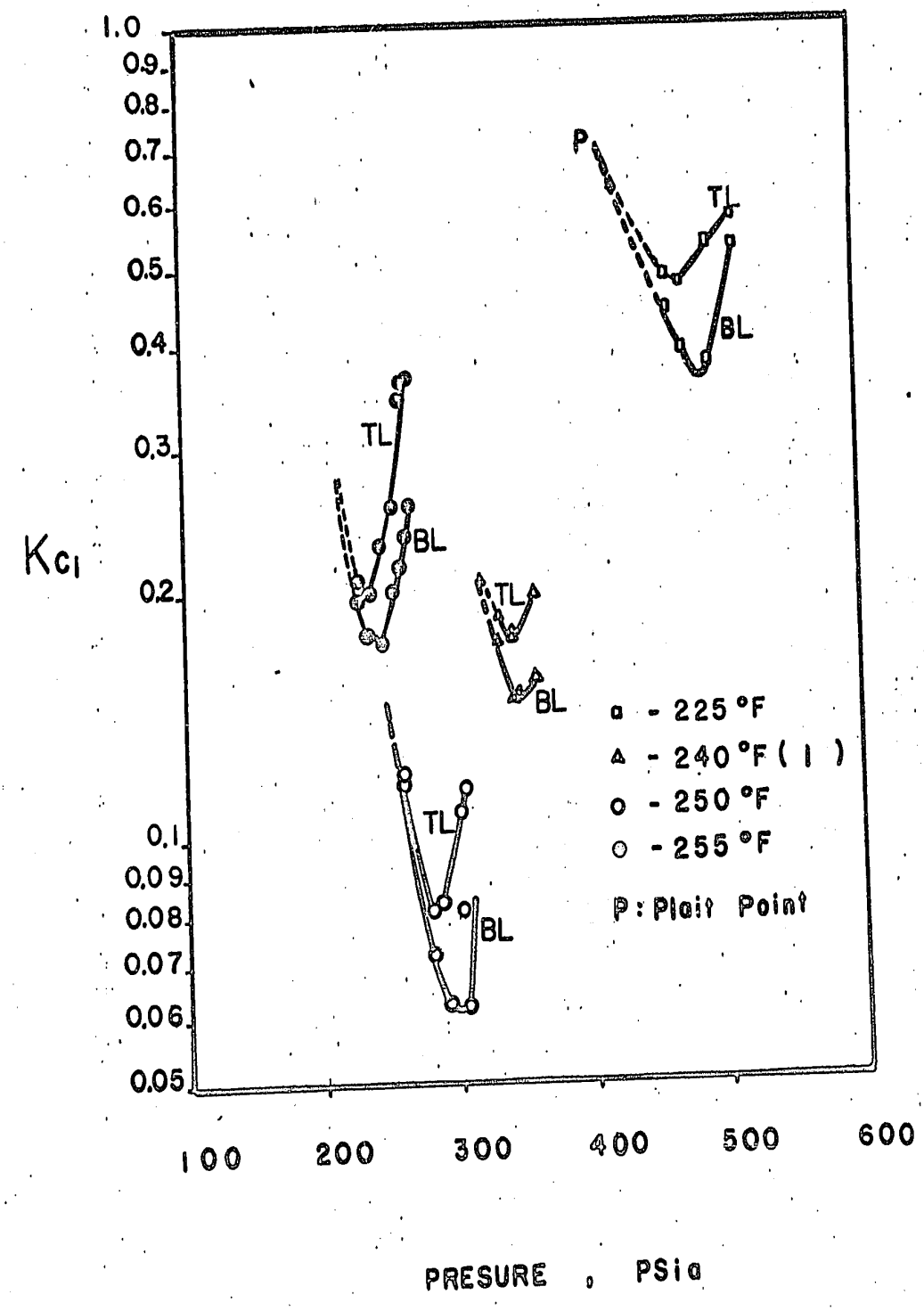

Figure 27. The K_{c_1}-P diagram for the nitrogen-methane-ethane system in the three-phase region.

DISCUSSION AND CONCLUSION

Nitrogen-Methane Mixtures

The pressure-composition data obtained in this investigation were compared with values seen in literature in Figures 4 and 5. Vapour-liquid equilibrium data for this system were reported by Bloomer and Parent (1). Graphically interpolation values from these values at -216.3 and -225.5°F were compared with the data obtained in this investigation.

Nitrogen-Ethane Mixture

The pressure-composition data obtained at -153.1°F are shown in Fig. 6. The agreement between the present data and that reported by Ellington et al.(4) at -150°F is very good. However, the values obtained in this investigation differ from that reported by Chang (10) at -151.1°F.

The -225.5°F isotherm obtained in this investigation disagrees with the data reported by Ellington et al.(4) at -225.1°F for the P-K curves, but it agrees fairly well with that reported by Cosway et al (3) at -220.5°F for the pressure-vapour composition curves. The pressure-composition data at -225.5°F are shown in Fig. 7.

It was found in this investigation that two liquid phases were present at temperatures lower than -218°F for the nitrogen-ethane binary and the nitrogen-methane ethane ternary. The compositions of the three coexisting phases are plotted as a function of equilibrium temperature in Fig. 19. The agreement between the data and that reported by Ellington et al.(4) and this work is very good at lower temperatures.

However, at -220°F, the data reported by Ellington et al. appear to be quite different from what one would expect from the present data. The concentration of ethane in the bottom liquid layer is usually higher than that in the top layer. The equilibrium ratio of K_{N_2}, which is defined as y_{N_2}/x_{N_2}, for the vapour-bottom liquid layer combination increases with the decreases of the equilibrium temperature while for the vapour top liquid layer combination decreases slightly with the decrease of the equilibrium temperature.

Nitrogen-Methane-Ethane Mixtures

For the vapour-liquid equilibrium, the results suggest that at constant temperature, K values of nitrogen always decrease with increase of pressure, and the K values of ethane decrease first with the increase of pressure, but as the total pressure approach a certain point, K values of ethane increase with the increase of total pressure. The K values of methane decrease with increase of pressure as the third parameter, $x_{CH_4}/(x_{CH_4} + x_{C_2H_6})$, less than 0.5, but as the third parameter increase, the K values decrease first with increase of pressure and then increase with the increase of total pressure.

It was necessary to adjust the volume of liquid in the cell to about two-third of the cell capacity to permit the observation of the liquid interface. Difficulty was encountered in keeping the liquid volume approximately constant and simultaneously keeping the methane and ethane ratio constant. For the pressure higher than 500 psia the solubility of nitrogen was high in liquid hydrocarbon mixture. While the hydrocarbon mixture was being fed two-third of the cell's capacity,

the liquid level will be risen and overflown out of the cell. Adjusting the hydrocarbon mixture's level to one-third capacity or less, the vapour and liquid phases in the equilibrium cell could be observed. The constant ratio of hydrocarbon mixture would not keep constant any more, since the hydrocarbon mixture vapourized in different ratio into vapour phase in equilibrium cell and volume regulator. In this work, however, only the data at 500 psia and below the ternary system of vapour-liquid equilibrium are presented.

In the partially miscible region, the partial solubility increases with the increases of temperatures. Along the liquid-liquid equilibrium curve, the pressure of the system decreases with the increase of methane concentration in the liquid at all the temperatures investigated. The concentration of nitrogen was very high in the vapour phase at all the temperatures. In all cases, the concentration of methane in the bottom liquid layer was always richer than that in the top liquid layer as indicated by the tie lines.

From the Figures 23 to 25, it is seen that at constant K'_H, $K'_H = \frac{(x_{c_1} + x_{c_2})_{(BL)}}{(x_{c_1} + x_{c_2})_{(TL)}}$, the lower the temperature, the lower the K'_{N_2} $K'_{N_2} = x_{N_2}(BL)/x_{N_2}(TL)$, values, i.e., the lower the concentration of nitrogen in bottom layer liquid. Same observation may be obtained at constant K'_{c_1} or K'_{c_2} conditions.

The separation of nitrogen from natural gases which are rich in nitrogen may be facilitated by taking advantage of the presence of two liquid phases at lower temperature.

APPENDIX I

Experimental and Smooth Data of the Systems Containing Nitrogen, Methane and Ethane.

TABLE 1.

Experimental Data For The System Nitrogen - Methane

Run No.	Temp. °F	Pressure psia	Composition, N_2 Mole Fraction	
			Liquid	Vapor
1	-216.3	102.8	0.0406	0.3425
2	-216.3	210.0	0.1960	0.6345
3	-216.3	309.0	0.3568	0.7369
4	-216.3	395.5	0.5269	0.7987
5	-216.3	465.0	0.6317	0.8382
6	-216.3	536.0	0.7663	0.8496
7	-216.3	553.0	0.8026	0.8561
8	-216.3	581.0	0.8340	0.8417
9	-216.3	588.0	0.8347	0.8340
10	-225.5	113.5	0.1323	0.5917
11	-225.5	139.0	0.1837	0.5658
12	-225.5	183.0	0.2537	0.6853
13	-225.5	243.0	0.3160	0.7467
14	-225.5	291.0	0.4639	0.8184
15	-225.5	336.5	0.5799	0.8497
16	-225.5	390.0	0.6985	0.8786
17	-225.5	435.5	0.7833	0.8937
18	-225.5	470.0	0.8498	0.9194
19	-225.5	519.0	0.9126	0.9379

TABLE XI

Experimental Data For The System Nitrogen - Ethane

Run No.	Temp. °F	Pressure psia	Composition, N_2 Mole Fraction	
			Liquid	Vapor
20	-153.1	40.5	0.0045	0.8405
21	-153.1	85.0	0.0201	0.9194
22	-153.1	153.0	0.0285	0.9496
23	-153.1	200.2	0.0337	0.9524
24	-153.1	305.0	0.0586	0.9618
25	-153.1	395.5	0.0845	0.9693
26	-153.1	500.0	0.1099	0.9707
27	-153.1	599.5	0.1621	0.9709
28	-153.1	709.0	0.2395	0.9705
29	-225.5	53.0	0.0140	0.9897
30	-225.5	107.0	0.0440	0.9958
31	-225.5	202.0	0.0879	0.9961
32	-225.5	300.0	0.1270	0.9960
33	-225.5	400.0	0.1835	0.9956
34	-225.5	500.0	0.2453	0.9940

TABLE III

Smoothed Data For The System Nitrogen - Methane

Temp. °F	Pressure psia	Composition, N_2 mol.fr. Liquid	Vapor	Equilibrium Constant K_{N_2}	K_{CH_4}
-216.3	76.7	0	0	-	-
-216.3	100.0	0.0457	0.3326	7.277	0.6993
-216.3	150.0	0.0946	0.4914	5.194	0.5617
-216.3	200.0	0.1809	0.6171	3.411	0.4674
-216.3	250.0	0.2623	0.6785	2.586	0.4358
-216.3	300.0	0.3507	0.7338	2.092	0.4099
-216.3	350.0	0.4344	0.7751	1.784	0.3976
-216.3	400.0	0.5249	0.8082	1.539	0.4037
-216.3	450.0	0.6073	0.8329	1.371	0.4255
-216.3	500.0	0.6889	0.8502	1.234	0.4815
-216.3	550.0	0.7845	0.8566	1.091	0.6654
-216.3	589.0	0.8345	0.8345	1.000	1.000
-225.5	53.4	0	0	-	-
-225.5	100.0	0.1023	0.5011	4.898	0.5557
-225.5	150.0	0.1997	0.6132	3.070	0.4093
-225.5	200.0	0.2884	0.7084	2.456	0.4098
-225.5	250.0	0.3719	0.7769	2.089	0.3952
-225.5	300.0	0.4958	0.8271	1.668	0.3429
-225.5	350.0	0.5999	0.8654	1.442	0.3364
-225.5	400.0	0.7172	0.8946	1.247	0.3727
-225.5	450.0	0.8091	0.9163	1.132	0.4984
-225.5	500.0	0.8843	0.9328	1.054	0.5808
-225.5	539.0	0.9401	0.9401	1.000	1.000

TABLE IV

Smoothed Data For The System Nitrogen - Ethane

Temp. °F	Pressure psia	Composition, N_2 mol.fr. Liquid	Vapor	Equilibrium Constant K_{N_2}	$K_{C_2H_6}$
-153.1	62.0	0	0	-	-
-153.1	100.0	0.0158	0.9274	58.69	0.0737
-153.1	150.0	0.0242	0.9482	39.18	0.0529
-153.1	200.0	0.0337	0.9524	28.26	0.0492
-153.1	250.0	0.0443	0.9571	21.60	0.0448
-153.1	300.0	0.0571	0.9627	16.86	0.0395
-153.1	350.0	0.0706	0.9655	13.67	0.0371
-153.1	400.0	0.0855	0.9696	11.34	0.0332
-153.1	450.0	0.0977	0.9701	9.929	0.0331
-153.1	500.0	0.1099	0.9707	8.832	0.0329
-153.1	550.0	0.1322	0.9708	7.343	0.0336
-153.1	600.0	0.1622	0.9710	5.986	0.0306
-153.1	650.0	0.1928	0.9707	5.034	0.0362
-153.1	700.0	0.2324	0.9706	4.176	0.0383
-225.5	0.187	0	0	-	-
-225.5	50.0	0.0211	0.9883	46.83	0.0119
-225.5	100.0	0.0412	0.9956	24.16	0.0045
-225.5	150.0	0.0628	0.9960	15.86	0.0042
-225.5	200.0	0.0859	0.9961	11.59	0.0042
-225.5	250.0	0.1083	0.9961	9.197	0.0043
-225.5	300.0	0.1309	0.9960	7.600	0.0046
-225.5	350.0	0.1557	0.9958	6.395	0.0049

TABLE IV (continued)

Temp. °F	Pressure psia	Composition, N_2 mol. fr. Liquid	Vapor	Equilibrium Constant K_{N_2}	$K_{C_2H_6}$
-225.5	400.0	0.1814	0.9956	5.488	0.0053
-225.5	450.0	0.2056	0.9953	4.841	0.0059
-225.5	500.0	0.2317	0.9948	4.293	0.0067
-225.5	550.0	0.2532	0.9935	3.923	0.0087
-225.5	600.0	0.2781	0.9913	3.564	0.0120

TABLE V.

Experimental Data For The Ternary System Nitrogen - Methane - Ethane at Temperature -225.5°F

Run No.	Pressure psia	Composition Liquid mol. fr. N_2	CH_4	C_2H_6	Composition Vapor mol.fr. N_2	CH_4	C_2H_6
36	73.7	0.0313	0.3063	0.6624	0.6075	0.3746	0.1089
37	150.0	0.0805	0.2935	0.6260	0.8471	0.1436	0.0093
38	200.0	0.0715	0.2790	0.6495	0.8580	0.1330	0.0090
39	229.0	0.1466	0.2635	0.5899	0.8967	0.0944	0.0089
40	300.0	0.2466	0.2369	0.5165	0.9016	0.0903	0.0081
41	300.0	0.1532	0.2597	0.5871	0.9153	0.0766	0.0081
42	345.0	0.2445	0.2305	0.5250	0.9283	0.0637	0.0080
43	415.0	0.3348	0.2053	0.4599	0.9381	0.0540	0.0079
44	50.0	0.0177	0.5479	0.4344	0.1917	0.6785	0.1298
45	100.0	0.0610	0.5237	0.4153	0.5223	0.4445	0.0332
46	148.9	0.1013	0.5011	0.3976	0.7442	0.2424	0.0134
47	201.0	0.1440	0.4761	0.3799	0.7501	0.2310	0.0101
48	252.2	0.2079	0.4428	0.3493	0.8462	0.1457	0.0081
49	283.0	0.5261	0.4142	0.3297	0.8539	0.1373	0.0090
50 *	344.0	0.4695	0.2953	0.2352	0.9276	0.0603	0.0121
51	393.0	0.4036	0.2864	0.2280	0.8591	0.1233	0.0176

TABLE V. (Continued)

Run No.	Pressure psia	Composition Liquid mol. fr. N_2	CH_4	C_2H_6	Composition Vapor mol.fr. N_2	CH_4	C_2H_6
52[a]	400.0	0.3741	0.3491	0.2768	0.9267	0.0571	0.0162
53	500.0	0.7299	0.1511	0.1190	0.9007	0.0819	0.0174
54	50.0	0.0133	0.6922	0.2945	0.1467	0.8361	0.0172
55	112.5	0.0868	0.6388	0.2744	0.2752	0.7099	0.0149
56	160.5	0.1413	0.6023	0.2564	0.7401	0.2553	0.0046
57	213.5	0.2086	0.5601	0.2313	0.7859	0.2111	0.0030
58	248.5	0.2863	0.5019	0.2118	0.8276	0.1649	0.0075
59	320.0	0.4028	0.4188	0.1784	0.8562	0.1314	0.0124
60	350.0	0.4818	0.3607	0.1575	0.8726	0.1138	0.0136
61[a]	400.0	0.5396	0.3225	0.1379	0.8543	0.1290	0.0167
62	500.0	0.7058	0.1951	0.0991	0.8765	0.1061	0.0171
63	55.0	0.0232	0.2267	0.7501	0.4514	0.3915	0.1571
64	104.3	0.0484	0.2207	0.7309	0.7682	0.1989	0.0329
65	156.0	0.0769	0.2140	0.7091	0.8797	0.1077	0.0126
66	202.0	0.1108	0.2087	0.6805	0.9021	0.0857	0.0122
67	250.0	0.1521	0.1965	0.6514	0.9199	0.0695	0.0106
68	300.0	0.1581	0.1967	0.6452	0.9254	0.0624	0.0122
69	422.0	0.2789	0.1665	0.5546	0.9363	0.0501	0.0136
70	51.5	0.0221	0.1121	0.8658	0.6347	0.2752	0.0901

TABLE V. (Continued)

Run No.	Pressure psia	Composition Liquid mol. fr. N_2	CH_4	C_2H_6	Composition Vapor mol. fr. N_2	CH_4	C_2H_6
71	101.0	0.0456	0.1102	0.8442	0.8499	0.1254	0.0247
72	151.0	0.0679	0.1094	0.8227	0.9112	0.0756	0.0132
73	197.0	0.0767	0.1044	0.8189	0.9389	0.0526	0.0085
74	200.0	0.0947	0.1062	0.7995	0.9385	0.0513	0.0084
75	290.0	0.1344	0.0983	0.7673	0.9547	0.0358	0.0095
76	300.0	0.1463	0.1029	0.7508	0.9578	0.0326	0.0096
77	400.0	0.2221	0.0841	0.6938	0.9690	0.0213	0.0097

@ The wrong data but make counts on these points.

TABLE VI

K Values For The Ternary System Nitrogen - Methane - Ethane

at Temperature = 225.5 °F

Run No.	Pressure psia	$\frac{x_{c_1}}{x_{c_1} + x_{c_2}}$	Equilibrium Constant K_{N_2}	K_{CH_4}	$K_{C_2H_6}$
29	53.0	0.0000	70.69	-	0.0104
30	107.0	0.0000	22.42	-	0.0044
31	202.0	0.0000	11.33	-	0.0042
32	300.0	0.0000	7.842	-	0.0046
33	400.0	0.0000	5.422	-	0.0054
34	500.0	0.0000	4.055	-	0.0069
70	51.5	0.1146	28.71	2.454	0.1040
71	101.0	0.1154	18.63	1.137	0.0292
72	151.0	0.1173	13.41	0.6910	0.0160
73	197.0	0.1131	12.24	0.5038	0.0103
74	200.0	0.1172	9.910	0.4830	0.0105
75	290.0	0.1135	7.103	0.3642	0.0123
76	300.0	0.1205	6.546	0.3168	0.0127
77	400.0	0.1081	4.362	0.2532	0.0139
63	55.0	0.2321	19.45	1.726	0.2094
64	104.3	0.2319	15.87	0.9012	0.0450
65	156.0	0.2318	11.43	0.5032	0.0177
66	202.0	0.2347	8.141	0.4106	0.0179

TABLE VI (Continued)

Run No.	Pressure psia	$\frac{x_{c_1}}{x_{c_1}+x_{c_2}}$	Equilibrium Constant K_{N_2}	K_{CH_4}	$K_{C_2H_6}$
67	250.0	0.2317	6.047	0.3536	0.0162
68	300.0	0.2336	5.853	0.3172	0.0189
69	422.0	0.2309	3.357	0.3009	0.0245
36	73.7	0.3162	19.40	1.222	0.0285
37	150.0	0.3192	10.52	0.4892	0.0148
38	200.0	0.3004	12.00	0.4767	0.0138
39	229.0	0.3087	6.116	0.3582	0.0151
40	300.0	0.3144	3.656	0.3811	0.0156
41	300.0	0.3067	5.974	0.2926	0.0138
42	345.0	0.3051	3.796	0.2763	0.0152
43	415.0	0.3086	2.801	0.2630	0.0172
44	50.0	0.5577	10.83	1.238	0.2988
45	100.0	0.5577	8.562	0.8487	0.0799
46	148.9	0.5576	7.946	0.4837	0.0377
47	201.0	0.5562	5.264	0.4868	0.0265
48	252.5	0.5590	4.070	0.3290	0.0291
49	289.0	0.5568	3.380	0.3914	0.0297
500	340.0	0.5566	1.975	0.2041	0.0514
51	393.0	0.5567	1.769	0.4305	0.0771
520	400.0	0.5577	2.477	0.1636	0.0565

TABLE VI (Continued)

Run No.	Pressure psia	$\frac{x_{c_1}}{x_{c_1}+x_{c_2}}$	Equilibrium Constant K_{N_2}	Equilibrium Constant K_{CH_4}	Equilibrium Constant $K_{C_2H_6}$
53	500.0	0.5594	1.230	0.5420	0.1062
54	50.0	0.7015	11.03	1.207	0.3001
55	112.5	0.6995	3.170	1.111	0.0583
56	160.5	0.7014	5.237	0.8238	0.0179
57	213.5	0.7077	3.767	0.3768	0.0129
58	248.5	0.7032	2.690	0.3285	0.0358
59	320.0	0.7012	2.125	0.3137	0.0695
60	350.0	0.6960	1.811	0.3155	0.0869
61b	400.0	0.7004	1.583	0.4000	0.1211
62	500.0	0.6691	1.241	0.5038	0.1783
10	113.5	1.000	0.609	0.5398	0
11	139.0	1.000	1.096	0.5912	0
12	189.0	1.000	2.701	0.6215	0
13	249.0	1.000	2.962	0.3703	0
14	291.0	1.000	1.764	0.3967	0
15	336.5	1.000	1.065	0.3977	0
16	350.0	1.000	1.697	0.0026	0
17	455.5	1.000	1.193	0.0951	0
18	470.0	1.000	1.067	0.5827	0
19	519.0	1.000	1.027	0.7174	0

TABLE VII

Experimental Data For The Ternary System Nitrogen – Methane – Ethane Containing Two Liquid Phases

Run No.	Temp. °F	Pressure psia	Composition Mole Fraction								
			Bottom Layer Liquid			Top Layer Liquid			Vapor		
			N_2	CH_4	C_2H_6	N_2	CH_4	C_2H_6	N_2	CH_4	C_2H_6
78	-225.5	551.0	0.4385		0.5615	0.9019		0.0983	0.9889		0.0111
79	-225.5	490.0	0.4488	0.1077	0.4435	0.8343	0.0763	0.0894	0.9469	0.0409	0.0122
80	-225.5	510.0	0.4313	0.0309	0.5378	0.8805	0.0286	0.0909	0.9728	0.0165	0.0107
81	-225.5	469.0	0.4624	0.1247	0.4129	0.7419	0.1036	0.1545	0.9372	0.0493	0.0135
82	-225.5	462.0	0.4804	0.1302	0.1545	0.7222	0.1185	0.1593	0.9282	0.0577	0.0141
83*	-250	309.5	0.1875		0.8125	0.9231		0.0769	0.9969		0.0031
84	-250	303.0	0.2926	0.0425	0.6649	0.8965	0.0217	0.0818	0.9916	0.0025	0.0059
85*	-250	283.0	0.3273	0.0835	0.5892	0.7958	0.0875	0.1172	0.9869	0.0071	0.0060
86	-250	258.4	0.4712	0.1625	0.3636	0.6435	0.1566	0.1999	0.9752	0.0188	0.0062

TABLE VII (Continued)

Run No.	Temp. °F	Pressure psia	Composition Mole Fraction: Bottom Layer Liquid H_2	CH_4	C_2H_6	Top Layer Liquid H_2	CH_4	C_2H_6	Vapor H_2	CH_4	C_2H_6
87	-250	304.4	0.2599		0.7401	0.9219		0.0781	0.9978		0.0022
88°	-250	270.5	0.4422	0.1601	0.3935	0.7185	0.1282	0.1533	0.9881	0.0094	0.0025
89	-250	304.7	0.2608		0.7392	0.9426		0.0574	0.9972		0.0028
90°	-250	287.0	0.3918	0.0904	0.5778	0.6395	0.0912	0.2693	0.9858	0.0081	0.0061
91	-250	284.0	0.3426	0.0907	0.5667	0.7749	0.0956	0.1265	0.9865	0.0075	0.0060
92°	-250	281.0	0.3414	0.0909	0.5677	0.7603	0.1014	0.1383	0.9868	0.0073	0.0059
93	-250	299.0	0.3130	0.0646	0.6224	0.8661	0.0482	0.0857	0.9947	0.0053	0.0050
94	-250	298.0	0.3165	0.0665	0.6270	0.8661	0.0476	0.0843	0.9904	0.0047	0.0049
95°	-250	299.5	0.3113	0.0673	0.6214	0.8619	0.0494	0.0887	0.9916	0.0040	0.0044
96	-240	377.5	0.3020		0.6980	0.9374		0.0626	0.9997		0.0003
97	-255	255.0	0.2781	0.0404	0.6815	0.8993	0.0321	0.0686	0.9889	0.0082	0.0039
98°	-255	242.0	0.3454	0.1273	0.5273	0.7913	0.0964	0.1123	0.9711	0.0214	0.0067

TABLE VII (Continued)

Run No.	Temp. °F	Pressure psia	Composition, Mole Fraction: Bottom Layer Liquid N_2	CH_4	C_2H_6	Top Layer Liquid N_2	CH_4	C_2H_6	Vapor N_2	CH_4	C_2H_6
99	-255	255.0	0.4661	0.1743	0.3596	0.6609	0.1574	0.1817	0.9597	0.0309	0.0094
100	-255	262.0	0.2696	0.0211	0.7093	0.9239	0.0136	0.0635	0.9921	0.0050	0.0029
101	-255	257.0	0.2744	0.0223	0.7033	0.9191	0.0148	0.0661	0.9914	0.0051	0.0035
102	-255	268.0	0.2627	0.0162	0.7211	0.9257	0.0111	0.0632	0.9932	0.0041	0.0027
103	-255	268.3	0.2508		0.7452	0.9444		0.0556	0.9999		0.0001
104[b]	-255	254.0	0.2763	0.0464	0.6773	0.8944	0.0317	0.0739	0.9879	0.0080	0.0041
105	-255	252.0	0.2804	0.0479	0.6717	0.8942	0.0329	0.0729	0.9876	0.0079	0.0045
106	-255	245.0	0.3224	0.1141	0.5635	0.8162	0.0861	0.0977	0.9741	0.0198	0.0061
107[b]	-255	222.0	0.5249	0.1782	0.2969	0.6125	0.1705	0.2170	0.9437	0.0445	0.0118
108[b]	-255	230.0	0.4879	0.1756	0.3365	0.6422	0.1597	0.1981	0.9519	0.0383	0.0098
109	-255	228.0	0.5042	0.1767	0.3191	0.6213	0.1676	0.2170	0.9554	0.0347	0.0099

TABLE VII (Continued)

Run No.	Temp. °F	Pressure psia	Composition, Mole Fraction: Bottom Layer Liquid H_2	CH_4	C_2H_6	Top Layer Liquid H_2	CH_4	C_2H_6	Vapor H_2	CH_4	C_2H_6
110°	-295	260.5	0.2744		0.7252	0.9371		0.0629	0.9999		0.0001
111°	-295	260.5	0.2549		0.7451	0.9429		0.0571	0.9999		0.0001

TABLE VIII

K Values and Distribution Coefficients For The Ternary System Nitrogen – Methane – Ethane

Containing Two Liquid Phases

Run No.	Equilibrium Ratio						Distribution Coefficient			
	Bottom Layer Liquid			Top Layer Liquid						
	K_{N_2}	K_{CH_4}	$K_{C_2H_6}$	K_{N_2}	K_{CH_4}	$K_{C_2H_6}$	K_{N_2}'	K_{C_1}'	K_{C_2}'	K_H'
78	2.235		0.0197	1.095		0.1129	0.4863		5.712	5.712
79	2.109	0.3797	0.0275	1.134	0.5360	0.1364	0.5379	1.411	4.961	3.326
80	2.235	0.5339	0.0199	0.104	0.5769	0.1177	0.4898	1.080	5.916	4.758
81	2.026	0.3953	0.0327	1.263	0.4758	0.0874	0.6232	1.203	2.672	2.083
82	1.932	0.4031	0.0362	1.285	0.4869	0.0885	0.6652	1.098	2.404	1.870
83[a]	5.316		0.0038	1.079		0.0403	0.2031		10.56	10.56
84	3.388	0.0598	0.0089	1.106	0.1152	0.0721	0.3264	1.958	8.128	6.834
85[a]	3.015	0.0830	0.0102	1.240	0.0811	0.0512	0.4113	0.9543	5.027	3.294
86	2.069	0.1157	0.0170	1.515	0.1200	0.0310	0.7322	1.037	1.819	1.483

TABLE VIII (Continued)

Run No.	Equilibrium Ratio						Distribution Coefficient			
	Bottom Layer Liquid			Top Layer Liquid						
	K_{H_2}	K_{CH_4}	$K_{C_2H_6}$	K_{N_2}	K_{CH_4}	$K_{C_2H_6}$	$K_{N_2'}$	$K_{C_1'}$	$K_{C_2'}$	$K_{H'}$
87	3.839		0.0029	1.082		0.0282	0.2819		9.476	9.476
88[a]	2.234	0.0573	0.0063	1.375	0.0733	0.0163	0.6154	1.280	2.566	1.981
89	3.823		0.0038	1.057		0.0488	0.2767		12.87	12.87
90[a]	2.971	0.0695	0.0105	1.541	0.0888	0.0226	0.5188	0.9912	2.145	1.853
91	2.879	0.0827	0.0105	1.273	0.0784	0.0474	0.4421	0.9487	4.479	2.920
92[a]	2.890	0.0803	0.0104	1.298	0.0719	0.0426	0.4490	0.8964	4.105	2.747
93	3.177	0.0820	0.0080	1.148	0.1099	0.0583	0.3614	1.340	7.262	5.130
94	3.129	0.0706	0.0078	1.143	0.0987	0.0581	0.3654	1.397	7.437	5.104
95[a]	3.103	0.0590	0.0071	1.150	0.0809	0.0496	0.3612	1.362	7.005	4.987
96	3.310		0.0004	1.066		0.0048	0.3221		11.18	11.18
97	3.555	0.2029	0.0057	1.099	0.2554	0.0568	0.3092	1.258	9.344	7.168

TABLE VIII (Continued)

Run No.	Equilibrium Ratio						Distribution Coefficient			
	Bottom Layer Liquid			Top Layer Liquid						
	K_{N_2}	K_{CH_4}	$K_{C_2H_6}$	K_{N_2}	K_{CH_4}	$K_{C_2H_6}$	K'_{N_2}	K'_{C_1}	K'_{C_2}	K'_{H}
98[a]	2.611	0.1681	0.0127	1.227	0.2219	0.0596	0.4365	1.320	4.695	3.136
99	2.039	0.1773	0.0261	1.452	0.1963	0.0517	0.7052	1.107	1.979	1.574
100	3.679	0.2369	0.0040	1.073	0.3676	0.0456	0.2918	1.551	11.17	9.598
101	3.612	0.2287	0.0049	1.078	0.3486	0.0529	0.2985	1.506	10.64	8.969
102	3.780	0.2531	0.0037	1.072	0.3694	0.0427	0.2838	1.459	11.09	9.923
103	3.924		0.0001	1.058		0.0018	0.2698		13.40	13.40
104[a]	3.575	0.1724	0.0060	1.104	0.2523	0.0555	0.3089	1.463	9.165	6.853
105	3.522	0.1649	0.0067	1.104	0.2401	0.0617	0.3136	1.456	9.214	6.801
106	3.021	0.1735	0.0108	1.193	0.2299	0.0624	0.3950	1.325	5.767	3.686
107[a]	1.797	0.2497	0.0397	1.5407	0.2609	0.0544	0.8569	1.045	1.368	1.226
108[a]	1.951	0.2181	0.0291	1.4822	0.2398	0.0494	0.7597	1.099	1.698	1.431

TABLE VIII (Continued)

Run No.	Equilibrium Ratio: Bottom Layer Liquid K_{H_2}	K_{CH_4}	$K_{C_2H_6}$	Equilibrium Ratio: Top Layer Liquid K_{H_2}	K_{CH_4}	$K_{C_2H_6}$	Distribution Coefficient K'_{H_2}	K'_{C_1}	K'_{C_2}	K'_{H}
109	1.090	0.1953	0.0310	1.537	0.2870	0.0456	0.8115	1.054	1.470	1.389
110	3.639		0.0001	1.057		0.0016	0.2931		11.53	11.53
111	3.922		0.0001	1.060		0.0017	0.2703		13.05	13.05

APPENDIX II

Calibration Results for the Thermocouple.

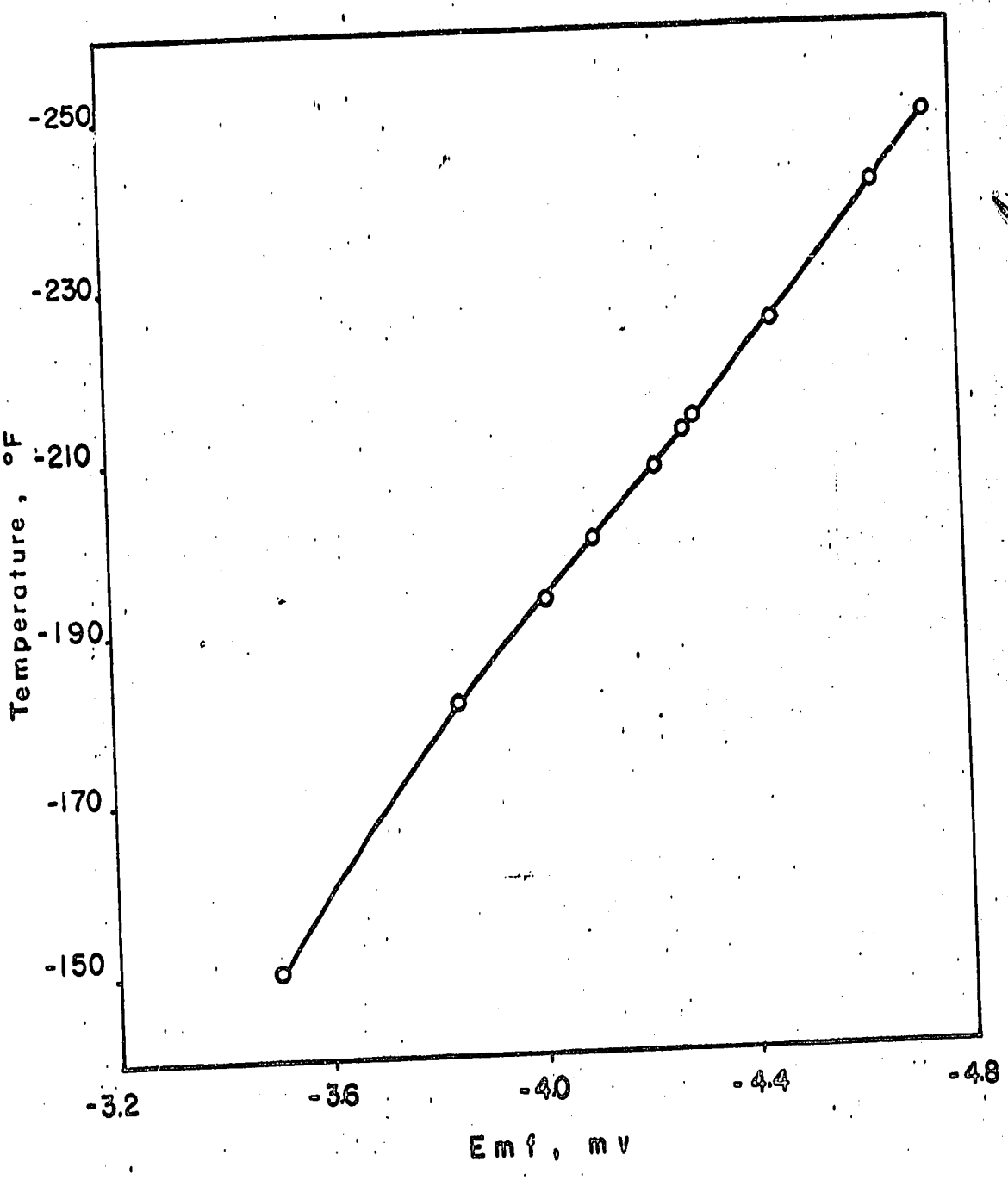

Figure 28. Calibration results of the thermocouple.

APPENDIX III

Calibration Curves.

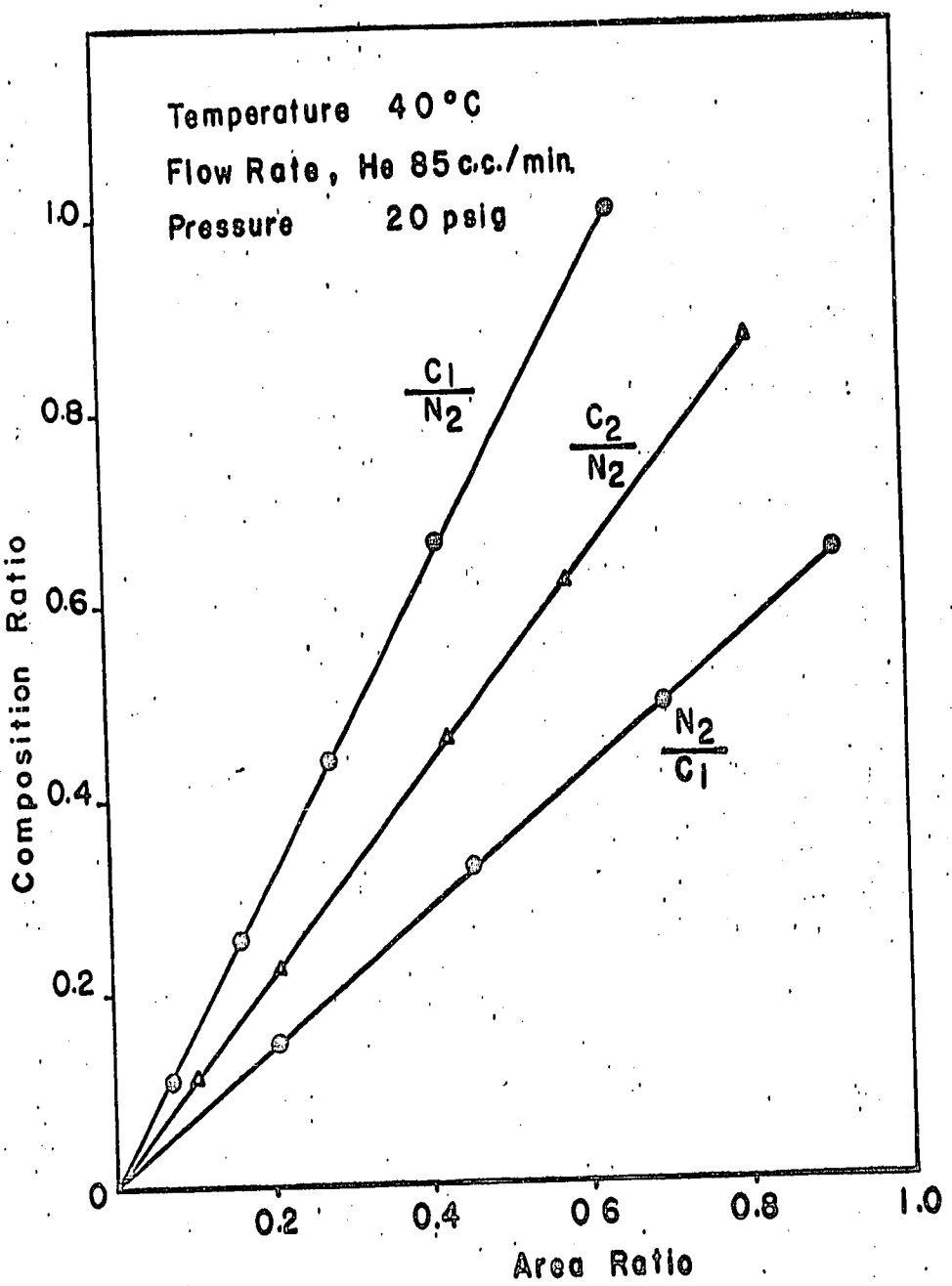

Figure 29. Calibration curves for the binary and the ternary mixtures.

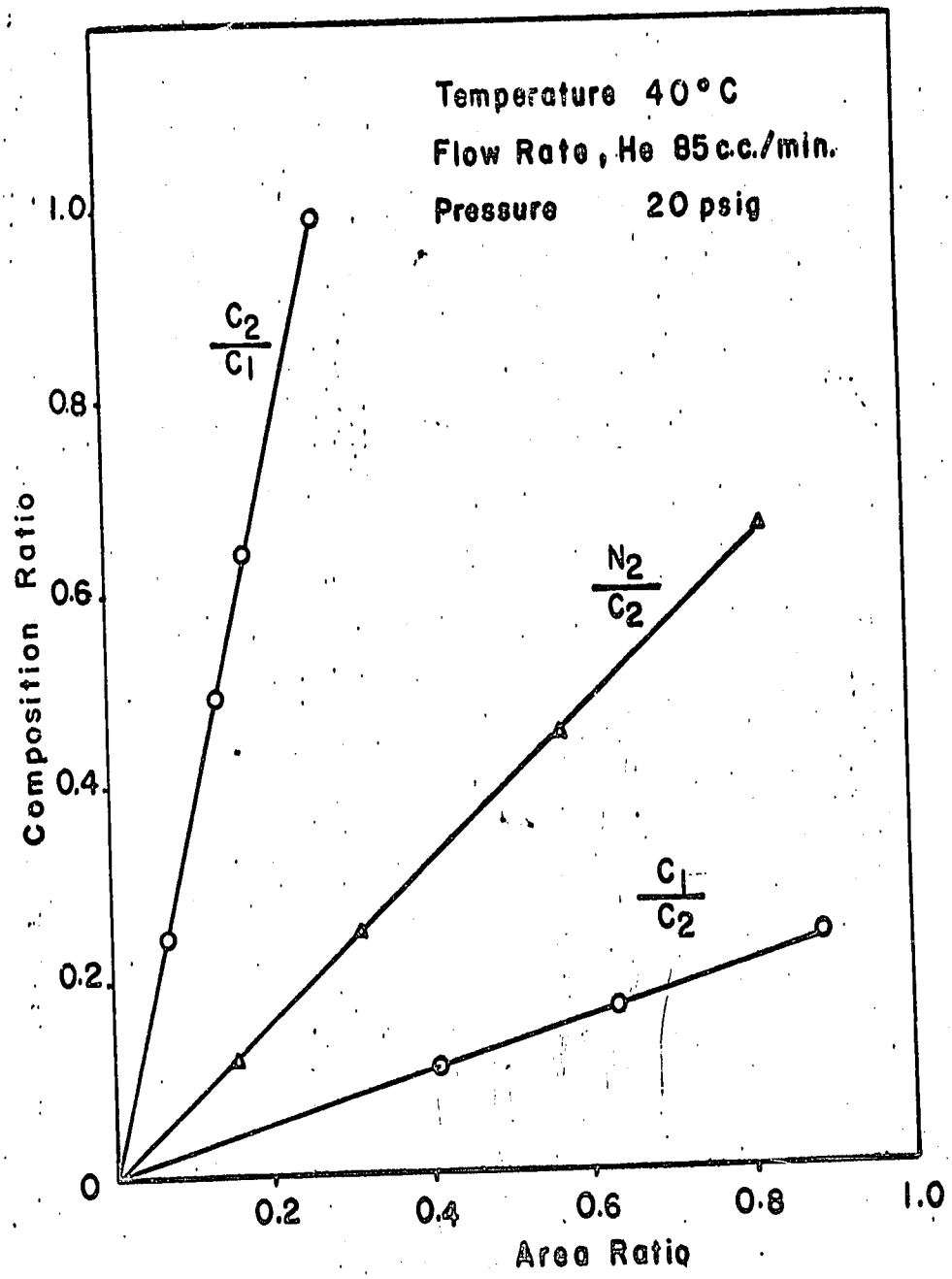

Figure 30. Calibration curves for the binary and the ternary mixtures.

BIBLIOGRAPHY

1. Bloomer, O.T. and J.D. Parent, Chem. Eng. Progr. Symposium Ser., No. 6, 49, 11 (1953).
2. Bloomer, O.T., D.C. Gami and J.D. Parent, Institute of Gas Technology Bulletin, No. 22 Chicago (1953).
3. Cosway, H.F. and D.L. Katz, A.I.Ch.E. Journal 5, 46 (1959).
4. Ellington, R.T., B.E. Eakin, J.D., Parent, D.C. Gami and O.T. Bloomer, Thermodynamic and Transport properties of Gases, Liquids and Solids, P. 180 (A.S.M.E.) McGraw Hill (1959).
5. Eakin, B.E., R.T. Ellington, and D.C. Gami, Institute of Gas Technology Research Bulletin No, 26 Chicago (1955).
6. McTaggart, H.A. and E. Edwards, Trans. Roy. Soc. Can., 13, Sec. III, 57 (1919).
7. Price, A.R. and R. Kobayashi, J. Chem. Eng. data, 4, 40 (1959).
8. Ruhemann, M., Proc. Roy. Soc., 171A, 121 (1939).
9. Cines, M.R., J.T. Roach, R.J. Hogan and C.H. Roland, Chem. Eng. Progr. Symposium Ser., No. 6, 49 (1953).
10. Chang, S.D., M.Sc. Thesis, University of Ottawa, May (1966).
    Chang, S.D., and B. C.-Y. Lu, Chem. Eng. Symposium Ser., No. 81 63, 181 (1967).
11. Stotler, H.H. and M. Benedict, Chem. Eng. Progr. Symposium Ser., No. 6, 49, 25 (1953).
12. Fedoritenko, A. and M. Ruhemann, Tech. Phys. (U.S.S.R.) 4, 36 (1937).

13. Bourbo, P. and I. Ischkin, Phys. Zeischrd. Sowjetunion, 10, 271 (1936).

14. Holst, G. and Hamburger, L., Zerlsch. f. Phys. Chemie, 91, 513 (1916).

15. Nederbragt, G.W., Ind. Eng. Chem., 30, 587 (1938).

16. Guter, M., D.M. Newitt, and M. Ruhemann, Proc. Roy. Soc. (A), 176, 140 (1940).

17. Sage, B.H. and W.N. Lacey, Ind. Eng. Chem., 26, 1218 (1934).

18. Ruhemann, M., Proc. Roy. Soc., 171A, 121 (1939).

19. Akers, W.W., Burns, J.F., Fairchild, W.R., Ind. Eng. Chem., 46, 2531 (1954).

20. Nederbragt, G.W., Ind. Eng. Chem., 30, 587 (1938).

21. Cheung, H. and D. I-J. Wang, Ind. Eng. Chem. Fundamentals, 3, 355 (1964).

22. Stockel, F., Phys. Zeischr d. Sowjetunion.

23. Kharakhorin, F.F., J. Tech. Phys. (U.S.S.R.), 11, 1133 (1941).

24. McCurdy, J.L. and D.L. Katz, Ind. Chem. Eng., 366, 75 (1944).

25. McKay, R.A., H.H. Reamer, B.H. Sage, Ind. Eng. Chem., 43, 2112 (1951).

26. Volva, J.M., J. Phys. Chem. (U.S.S.R.), 14, 260 (1940).

27. Sage, B.H. and W.N. Lacey, Ind. Eng. Chem., 26, 1036 (1934).

28. Stockel, F. and N. Zinn, Zhurnal Khimicheskon Promyshlennosti, 16, No. 8 (1939).

13. Bourbo, P. and I. Ischkin, Phys. Zeischrd. Sowjetunion, 10, 271 (1936).

14. Holst, G. and Hamburger, L., Zerisch. f. Phys. Chemie, 91, 513 (1916).

15. Nederbragt, G.W., Ind. Eng. Chem., 30, 567 (1938).

16. Guter, M., D.M. Newitt, and M. Ruhemann, Proc. Roy. Soc. (A), 176, 140 (1940).

17. Sage, B.H. and W.N. Lacey, Ind. Eng. Chem., 26, 1218 (1934).

18. Ruhemann, M., Proc. Roy. Soc., 171A, 121 (1939).

19. Akers, W.W., Burns, J.F., Fairchild, W.R., Ind. Eng. Chem., 46, 2531 (1954).

20. Nederbragt, G.W., Ind. Eng. Chem., 30, 587 (1938).

21. Cheung, H. and D. I-J. Wang, Ind. Eng. Chem. Fundamentals, 3, 355 (1964).

22. Stockel, F., Phys. Zeischr d. Sowjetunion.

23. Kharakhorin, F.F., J. Tech. Phys. (U.S.S.R.), 11, 1133 (1941).

24. McCurdy, J.L. and D.L. Katz, Ind. Chem. Eng., 366, 75 (1944).

25. McKay, R.A., H.H. Reamer, B.H. Sage, Ind. Eng. Chem., 43, 2112 (1951).

26. Volva, J.M., J. Phys. Chem. (U.S.S.R.), 14, 268 (1940).

27. Sage, B.H. and W.N. Lacey, Ind. Eng. Chem., 26, 1036 (1934).

28. Stoetol, F. and N. Zinn, Zhurnal Khimicheskon Promyshlennosti, 16, No. 8 (1939).

29. Ruhemann, M. and N. Zinn, Phys. Zeitschr. d. Sowjetunion, 12, 369 (1937).

30. Stutzman, L.F. and G.F. Brown, Chem. Eng. Progr., 45, 139 (1949).

31. Inglis, J. Phil. Mag. VI, 11, 640 (1906).

32. Dodge B.F. and A. Duhar, J. Amer. Chem. Soc., 49, 591 (1927).

33. Torocheshnikov, N.S., Journ. Techn. Phys. (U.S.S.R.), 7, 1107 (1937).

34. Aroyan, H.F. and D.L. Katz, Ind. Eng. Chem., 43, 185 (1951).

35. Davis, J.A., N. Rodewald and F. Kureta, Ind. Eng. Chem., 55, 539 (1963).

36. Armstrong G.T., RNBS. Vol. 55 No. 1 (1955) June.

37. Conversion Tables for Honeywell Pyrometers, P. 16 (1964).

38. Stormer, C.J., Rev. Sci. Instr., 31, 1159 (1960).

END OF REEL